

AD-A264 810



DOCUMENTATION PAGE

OMB No 0704-0188

ation estimated to affect 1 hour per response, including the time for reviewing instructions, searching existing data sources, gathering and reviewing the collection of information. Send comments regarding this burden estimate or any other aspect of this reducing this burden to Washington Headquarters Services, Directorate for Information Operations and Reports, 415 Jefferson 2, and to the Office of Management and Budget, Paperwork Reduction Project (0704-0188), Washington, DC 20503.

2. REPORT DATE May 1993		3. REPORT TYPE AND DATES COVERED Technical (6/1/92-5/31/93)		(2)
4. TITLE AND SUBTITLE An Extension of a Kinetic Theory of Polymer Crystallization Through the Exclusion of Negative Barriers			5. FUNDING NUMBERS N00014-91-J-1078	
6. AUTHOR(S) J.I. Scheinbeim, L. Petrone and B.A. Newman				
7. PERFORMING ORGANIZATION NAME(S) AND ADDRESS(ES) Department of Mechanics and Materials Science College of Engineering, Rutgers University P.O. Box 909 Piscataway, NJ 08855-0909			8. PERFORMING ORGANIZATION REPORT NUMBER #27	
9. SPONSORING / MONITORING AGENCY NAME(S) AND ADDRESS(ES) Dr. JoAnn Milliken Office of Naval Research Arlington, VA 22217-5000			10. SPONSORING / MONITORING AGENCY REPORT NUMBER	
11. SUPPLEMENTARY NOTES Macromolecules <u>26</u> , 933-945 (1993).				
12a. DISTRIBUTION / AVAILABILITY STATEMENT Approved for public release; distribution unlimited. Reproduction in whole or in part is permitted for any purpose of the United States Government.				
13. ABSTRACT (Maximum 200 words) The simplest version of the Lauritzen-Hoffman (LH) model of polymer crystallization, which applies to infinitely long model polymer molecules crystallizing on an existing substrate of infinite width, is reexamined. The mathematical expressions for the model free energy barriers are observed to take on negative values at high supercooling. Since such negative barriers appear to be physically unrealizable for the crystallization process, the LH model is extended by imposing a mathematical constraint on the expressions for the barriers, to forbid them from ever being negative. The extended model contains one parameter γ which varies from 0 to 1 and is analogous to the parameter ψ of the LH model. For all values of γ less than 1, the extended model predicts a finite lamellar thickness at every supercooling; moreover, this thickness at large undercooling, decreases monotonically with increasing undercooling, in agreement with experiment but in marked contrast to the LH model which exhibits the well-known δ catastrophe. The relative insensitivity of the calculated lamellar thicknesses to the parameter γ supports the use of $\gamma = 0$ as a first approximation for mathematical convenience in practice.				
14. SUBJECT TERMS			15. NUMBER OF PAGES 51	
			16. PRICE CODE	
17. SECURITY CLASSIFICATION OF REPORT UNCLASSIFIED	18. SECURITY CLASSIFICATION OF THIS PAGE	19. SECURITY CLASSIFICATION OF ABSTRACT	20. LIMITATION OF ABSTRACT	

OFFICE OF NAVAL RESEARCH

Contract N00014-91-J-1078

Technical Report No. 27

**AN EXTENSION OF A KINETIC THEORY OF POLYMER CRYSTALLIZATION
THROUGH THE EXCLUSION OF NEGATIVE BARRIERS**

by J.I. Scheinbeim, L. Petrone and B.A. Newman

Macromolecules

Department of Mechanics and Materials Science
College of Engineering
Rutgers University
Piscataway, NJ 08855-0909

Accession For	
NTIS CRA&I	<input checked="checked" type="checkbox"/>
DTIC TAB	<input type="checkbox"/>
Unannounced	<input type="checkbox"/>
Justification	
By	
Distribution /	
Availability Codes	
Dist	Avail and/or Special
A-1	

May 1993

Reproduction in whole or in part is permitted for any purpose of the United States Government

This document has been approved for public release and sale; its distribution is unlimited

AN EXTENSION OF A KINETIC THEORY OF POLYMER CRYSTALLIZATION THROUGH THE
EXCLUSION OF NEGATIVE BARRIERS

Jerry I. Scheinbeim, Louis Petrone, Brian A. Newman
Department of Mechanics and Materials Science
Rutgers University
Piscataway, NJ 08855-0909

ABSTRACT

The simplest version of the Lauritzen-Hoffman (LH) model of polymer crystallization which applies to infinitely long model polymer molecules crystallizing on an existing substrate of infinite width, is re-examined. The mathematical expressions for the model free energy barriers are observed to take on negative values at high supercooling. Since such negative barriers appear to be physically unrealizable for the crystallization process, the LH model is extended by imposing a mathematical constraint on the expressions for the barriers, to forbid them from ever being negative. The extended model contains one parameter γ which varies from zero to one and is analogous to the parameter ψ of the LH model. For all values of γ less than one, the extended model predicts a finite lamellar thickness at every supercooling; moreover, this thickness, at large undercooling, decreases monotonically with increasing undercooling in agreement with experiment, but in marked contrast to the LH model which exhibits the well-known δl catastrophe. The relative insensitivity of the calculated lamellar thicknesses to the parameter γ supports the use of $\gamma = 0$ as a first approximation for mathematical convenience in practice.

I. INTRODUCTION

Recently, the crystallization of poly(vinylidene) fluoride (PVF_2) in the presence of high electric fields has been studied both experimentally and theoretically. Of the four well-known crystalline forms α , β , γ , and δ (or II, I, III, and IV) of PVF_2 , the phase with the largest spontaneous polarization and potential for applications is the β -phase.

Crystallization of PVF_2 from a concentrated solution of tricresyl phosphate in the presence of a high electric field was observed¹ to produce β -phase crystals, with dipoles oriented in the field direction, during the initial stages of crystallization followed by the growth of unoriented α -crystals (non-polar) as crystallinity increased and the tricresyl phosphate content decreased by evaporation. The decrease in tricresyl phosphate content and subsequent crystal growth behavior suggests that the local electric field in the solution region changes. Other experimental and theoretical^{2,3} studies of crystallization of PVF_2 from the melt in the presence of a high static electric field have been made, and were found to give γ -phase crystals which however did not show crystal orientation. As part of the continuing effort to understand the structure-property relationships of PVF_2 and because of its practical importance, our ultimate goal--despite the complexity of the system described--is to develop a theory or model which can account for its crystallization behavior from concentrated solutions in the presence of an electric field.

As in the case of isothermal crystallization of α and γ phase from the melt in an electric field,³ a theory of isothermal crystallization of α , β , and δ phase from concentrated solution in an electric field, would be based on "classical" and "polymer" theories of nucleation and growth in the absence of an applied field. Most importantly, the nucleation barrier or activation free energy barrier for nucleation would certainly be different in the presence of the field than in its absence; and this barrier has been seen to be of fundamental importance in the theories of polymer crystallization, the simplest of which is the LH or Lauritzen-Hoffman theory.^{4,5} One possibly

unrealistic feature which seems to have been incorporated into the LH theory in order to simplify it, is that the nucleation barrier is not constrained in the theory to take on only nonnegative values.⁶ The word "barrier" connotes a positive quantity, and furthermore, the LH theory is based on transition state theory in which the barrier corresponds to an intermediate configuration or transition state of the system which is at a free energy maximum relative to some initial and final state of the system.⁹ Moreover, the LH theory exhibits, in contrast with experiment, the δl catastrophe wherein the calculated average lamellar thickness \bar{l} suddenly passes through a minimum and becomes infinite at a temperature, T_c , corresponding to a moderately large undercooling; and, in fact, the nucleation barrier in this theory is positive for all $T > T_c$, is zero at $T = T_c$, and is negative for all $T < T_c$ for the special case which Lauritzen and Hoffman^{4,5} have recently considered. Therefore, prior to developing an extension of the LH theory which would involve ascertaining the effect of an electric field on the nucleation barrier, we try to extend the LH theory to larger undercooling by incorporating into it the assumption that free energy barriers cannot be negative. Note that, unlike in the LH theory of polymer crystallization, barriers in classical nucleation theory are never negative; however, the classical theory does not explicitly take into account polymer chain folding, and for that reason, we have not yet considered modifying the Marand and Stein theory² of crystallization from the melt to treat the PVF₂/tricresyl phosphate crystallizing solution.

The remainder of this paper is organized as follows. In Section II, the LH model is described. The kinetic treatment of the LH model is given in Section III. The rate constants needed for this treatment are determined in Section IV. Next, our extension of the LH model is described in Section V; the conditions which determine the sign of $\Delta\phi_1$, the free energy of formation of that portion of a model polymer molecule which crystallizes first on an existing crystal, are found in Section VI. A summary of the expressions for the barriers in our model is given in Section VII along with the expressions

for the average lamellar thickness. In Section VIII, the variable transformations required as a preliminary to numerical integration are introduced. Results and discussion appear in Section IX, and conclusions are given in Section X.

II. THE LAURITZEN-HOFFMAN MODEL

The model to be extended is one version^{4,5} of the well-known Lauritzen-Hoffman (LH) model of polymer crystallization. Our description of this version is as follows. The model polymer molecules are assumed to be infinitely long and crystallize on an existing crystalline face or substrate which is assumed to be infinitely wide (i.e. the fact that its width is finite is ignored). A sequence of length l of polymer segments of width a and thickness b as well as the volume associated with that sequence--which is taken to be a parallelepiped of length l , width a , and thickness b --is designated as a stem. Only stems of length l can crystallize on an existing face of length l , but the length l , the lamellar thickness, can vary from crystal to crystal. Any sequence of length l of segments of a model molecule can be placed first on a given face and, upon placement, is designated as the first stem. The free energy of formation of the first stem is

$$\Delta\phi_1 - \Delta\phi_0 = \Delta\phi_1 - 0 \quad \text{or} \quad \Delta\phi_1 = 2ab\sigma'_e + 2bl\sigma - abl\Delta f$$

where $\Delta f > 0$ is the free energy of fusion per unit volume at a temperature T below the melting point T_m^* of the model polymer (i.e. of a crystal of very large l) and $\Delta f = 0$ at $T = T_m^*$; where σ is the lateral surface free energy per unit area (i.e. that associated with the surfaces of area bl and al of a stem); and where σ'_e is the surface free energy per unit area associated with the cilium that protrudes through each of the surfaces of area ab of the first stem. Recently,⁴⁻⁷ σ'_e has been assumed to be zero; generally, one can assume¹¹ that $0 \leq \sigma'_e \leq \sigma_e$. All surface free energies per unit area in the model are assumed to be independent of T and l . (See Figure 2(a) of Reference

4 or Figure 22 of Reference 5.) The placement of each subsequent stem involves:

1. the destruction of the cilium associated with one of the surfaces of area ab of an adjacent stem already crystallized,
2. an adjacent reentry and the formation of a tight fold associated with two surfaces of area ab , and
3. the formation of a cilium associated with the remaining surface of area ab of the stem being placed.

Only adjacent reentry and hence only tight folding is incorporated in this version of the model.

The free energy of formation of the ν th stem ($\nu > 1$) is therefore

$$\Delta\phi_\nu - \Delta\phi_{\nu-1} = -ab\sigma'_e + 2ab\sigma_e + ab\sigma'_e - abl\Delta f$$

or

$$\Delta\phi_\nu - \Delta\phi_{\nu-1} = 2ab\sigma_e - abl\Delta f = -E$$

where $\Delta\phi_\nu$ is the free energy of formation of a group of ν stems (relative to $\Delta\phi_0 = 0$) and where σ_e is the surface free energy per unit area associated with half of a fold. Iteration of $\Delta\phi_\nu - \Delta\phi_{\nu-1} = -E$ ($\nu > 1$) gives

$$\begin{aligned}\Delta\phi_\nu &= \Delta\phi_1 - (\nu-1)E \\ &= 2bl\sigma + 2ab\sigma'_e - 2ab\sigma_e + \nu ab(2\sigma_e - l\Delta f).\end{aligned}$$

In order that stem additions subsequent to the placement of the first stem be thermodynamically favorable, i.e. in order that they would in fact occur, one must impose the constraint $-E < 0$ and consequently $l > \frac{2\sigma_e}{\Delta f}$. Stems of smaller length are unstable and disappear. By contrast, $\Delta\phi_1$ can be positive, zero,

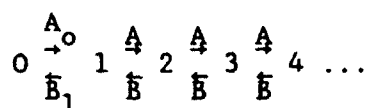
or negative; $E > 0$ guarantees that $\Delta\phi_\nu < 0$ will occur for finite ν . Note the sign conventions for $\Delta\phi_1$ and E .

III. THE KINETIC TREATMENT OF THE LAURITZEN-HOFFMAN MODEL

Our description of the kinetic treatment^{4,5} of the LH model is as follows. The following assumptions are made:

1. Assume that transition state theory can be utilized to describe the kinetics of the LH model of polymer crystallization.
2. Assume that the formation (crystallization) of a single stem is an elementary process or elementary reaction; that the destruction (melting) of a single stem is an elementary process or elementary reaction; and that transition state theory can be applied to these two elementary processes with a single transition state corresponding to a relative free energy maximum or barrier thus occurring between each two integral values of ν on a plot of $\Delta\phi_\nu$ vs. ν .
3. Assume that only one stem at a time can be formed or destroyed.

The kinetic problem is to derive an expression for the net rate $S_\nu(\ell, T)$ at which stems of length ℓ (and width a) pass over or surmount the ν th free energy barrier at temperature T . The problem requires consideration of the following set of connected elementary reactions



where A is the rate constant for the forward reaction $\nu \rightarrow \nu+1$ ($\nu \geq 1$) and B is that for the reverse reaction $\nu+1 \rightarrow \nu$ ($\nu \geq 1$), and where A_0 and B_1 are the analogous rate constants for the $\nu=0 \rightarrow \nu=1$ reactions. Solution⁸ of this problem in the steady-state approximation gives

$$S_\nu(\ell, T) = \frac{N_0 A_0 (A - B)}{A - B + B_1} = S(\ell, T)$$

for all ν , where N_0 is the number of sites or locations available for the placement of a first stem. The total net rate at which stems (i.e. the net rate including stems of all possible values of l) pass over the ν th barrier at temperature T is given, for all ν , by

$$S_{\text{Total}}(T) = \sum_{l=l_1}^{\infty} S(l, T)$$

where l_1 is the smallest allowed value of l which satisfies the constraint $l > \frac{2\sigma_e}{\Delta f}$. Note that l is a discrete variable--the smallest increment in l that can be made is the monomer repeat length l_u . To find l_1 , first write $l = ml_u$, where m is a positive integer. Then $l > \frac{2\sigma_e}{\Delta f}$ implies $m > \frac{2\sigma_e/\Delta f}{l_u}$, that is, m is greater than or equal to the smallest integer greater than $\frac{2\sigma_e/\Delta f}{l_u}$, and therefore, $l_1 = [1 + \text{INT}(X)]l_u$, where $X = \frac{2\sigma_e/\Delta f}{l_u}$ and $\text{INT}(X)$ designates the integer part of X . Substituting $l_u = \frac{2\sigma_e}{X\Delta f}$ into the expression for l_1 gives $l_1 = \left[\frac{1 + \text{INT}(X)}{X} \right] \left(\frac{2\sigma_e}{\Delta f} \right)$. To a good approximation, $\frac{1 + \text{INT}(X)}{X} \approx 1$ (i.e. X is sufficiently greater than 1) so that $l_1 \approx \frac{2\sigma_e}{\Delta f}$.

Finally, one assumes that $\sum_{l=l_1}^{\infty} S(l, T) \approx \frac{1}{l_u} \int_{l_1}^{\infty} S(l, T) dl$; and the

kinetically-determined average lamellar thickness is then given by

$$l(T) = \frac{\int_{l_1}^{\infty} l S(l, T) dl}{\int_{l_1}^{\infty} S(l, T) dl}.$$

IV. DETERMINATION OF THE RATE CONSTANTS

To obtain expressions for A_0 , B_1 , A and B , one must first determine expressions for the free energy barriers for the relevant reactions $\nu \xrightarrow{\pm} \nu+1$ ($\nu \geq 0$). Let E_1 be the free energy barrier to the destruction of the first stem; then $\Delta\phi_1 + E_1$ is the barrier to the formation of the first stem in order that $(\Delta\phi_1 + E_1) - E_1 = \Delta\phi_1$. Let E_2 be the free energy barrier to the formation of

each subsequent stem; then $E + E_2$ is the barrier to the destruction of each such stem in order that $(E + E_2) - E_2 = E$. Now, one does not know the free energy barrier to the formation of the first stem. At least, one does know that it depends on what length l' of a fully adsorbed stem of length l actually crystallizes before the barrier is surmounted. If $l' = 0$, then none of the free energy of crystallization (i.e. $-abl\Delta f$) is released before the barrier is surmounted, and clearly, $\Delta\phi_1 + E_1 = 2ab\sigma'_e + 2bl\sigma$ and $E_1 = abl\Delta f$. In general then, for $0 \leq l' \leq l$,

$$\Delta\phi_1 + E_1 = 2ab\sigma'_e + 2bl\sigma - abl'\Delta f \quad \text{and} \quad E_1 = ab(l-l')\Delta f.$$

Since l' is unknown, a parameter $\psi = \frac{l'}{l}$ with $0 \leq \psi \leq 1$, is introduced in order that all possible so-called apportionments of the free energy of fusion $abl\Delta f$ between the rate constants for the formation and destruction of a first stem (i.e. for the forward and reverse reactions $0 \rightleftharpoons 1$) can be considered. Thus,

$$\Delta\phi_1 + E_1 = 2ab\sigma'_e + 2bl\sigma - \psi abl\Delta f \quad \text{and} \quad E_1 = (1-\psi) abl\Delta f.$$

Note that the greater the amount $\psi abl\Delta f$ of the free energy of fusion which is in fact "apportioned" (i.e. the greater the value of ψ or l'), the smaller the value of both $\Delta\phi_1 + E_1$ and E_1 (for a given l and T). A very similar interpretation of ψ has been discussed recently.⁷

Similarly, for each subsequent stem, let l'' ($0 \leq l'' \leq l$) be the length of a fully adsorbed stem which actually crystallizes before the barrier to the formation of the stem is surmounted. Then

$$E_2 = 2ab\sigma_e - abl''\Delta f \quad \text{and} \quad E + E_2 = ab(l-l'')\Delta f.$$

Define the apportionment parameter $\hat{\psi} = \frac{l''}{l}$ with $0 \leq \hat{\psi} \leq 1$ so that

$$E_2 = 2ab\sigma_e - \hat{\psi} abl\Delta f \quad \text{and} \quad E + E_2 = (1-\hat{\psi}) abl\Delta f.$$

Finally, utilizing transition state theory,

$$A_0 = \frac{kT}{h} e^{-(\Delta\phi_1 + E_1 + \Delta\hat{F})/kT} = \beta e^{-(\Delta\phi_1 + E_1)/kT}$$

$$B_1 = \beta e^{-E_1/kT} ; A = \beta e^{-E_2/kT} ; B = \beta e^{-(E+E_2)/kT}$$

where $\Delta\hat{F}$ is the contribution to each barrier as a result of retardations in the transport of a polymer chain through the liquid to the substrate or vice versa. Note that $\frac{B}{A}$ does not depend on $\hat{\psi}$ and that $\frac{B_1}{A_0}$ does not depend on ψ as required.

V. THE EXTENSION OF THE LAURITZEN-HOFFMAN MODEL

As implied throughout the above discussion, the application of transition state theory to the elementary processes of single stem formation and destruction presumes that there is a single relative free energy maximum⁹ or barrier between each two integral values of ν on a plot of $\Delta\phi_\nu$ vs. ν . Consequently, $\Delta\phi_1 + E_1$, E_1 , E_2 , and $E + E_2$ should never be negative. Clearly, $E_1 = (1-\psi)abl\Delta f$ and $E + E_2 = (1-\hat{\psi})abl\Delta f$ are never negative; however, the expressions given above for $\Delta\phi_1 + E_1$ and E_2 can be negative. In fact, E_2 , for example, is negative for all l such that $\frac{2\sigma_e}{\hat{\psi}\Delta f} < l$ for a given Δf , $\hat{\psi}$, and σ_e . We propose to extend the LH model by incorporating into the model the assumption that free energy barriers cannot be negative, i.e. only apportionments of the free energy of fusion which result in a nonnegative barrier will be allowed.

In order to incorporate this constraint into the model, first note that $\Delta\phi_1 + E_1 = 2ab\sigma'_e + 2bl\sigma - \psi abl\Delta f$ is never negative when $\Delta\phi_1$ is positive since then, $abl\Delta f < 2ab\sigma'_e + 2bl\sigma$ always holds and $\psi abl\Delta f < 2ab\sigma'_e + 2bl\sigma$ follows. However, when $\Delta\phi_1$ is negative, the expression $2ab\sigma'_e + 2bl\sigma - \psi abl\Delta f$ can be negative. The requirement that $\Delta\phi_1 + E_1 \geq 0$ hold when $\Delta\phi_1$ is negative implies that one is not allowed to apportion all of the free energy of fusion $abl\Delta f$ when $\Delta\phi_1$ is negative. If the amount $\psi abl\Delta f$ of the free energy of fusion which is apportioned were to exceed $2ab\sigma'_e + 2bl\sigma$, then $\Delta\phi_1 + E_1$ would be negative.

The maximum amount which can be apportioned is indeed $2ab\sigma'_e + 2bl\sigma$, and therefore one has, when $\Delta\phi_1 < 0$,

$$\Delta\phi_1 + E_1 = \xi(2ab\sigma'_e + 2bl\sigma)$$

where ξ is an apportionment parameter with $0 \leq \xi \leq 1$. Using $(\Delta\phi_1 + E_1) - E_1 = \Delta\phi_1$ or $E_1 = (\Delta\phi_1 + E_1) - \Delta\phi_1$ gives

$$E_1 = \xi(2ab\sigma'_e + 2bl\sigma) - (2ab\sigma'_e + 2bl\sigma - abl\Delta f) = abl\Delta f - (1-\xi)(2ab\sigma'_e + 2bl\sigma).$$

Observe that the requirement that $\Delta\phi_1 + E_1 \geq 0$ holds when $\Delta\phi_1$ is negative is equivalent to the physically realistic requirement that the barrier E_1 to the destruction of the first stem cannot be smaller than the free energy increase $(-\Delta\phi_1)$ that occurs upon its destruction. Note that $abl\Delta f - (2ab\sigma'_e + 2bl\sigma) = -\Delta\phi_1$. Also, this physically realistic requirement implies that an adsorbed first stem cannot completely crystallize before the barrier to the formation of that stem is surmounted, i.e. that the upper limit on ℓ' is less than ℓ when $\Delta\phi_1$ is negative. This upper limit on ℓ' is determined later. For $\Delta\phi_1 > 0$, the expressions $\Delta\phi_1 + E_1 = 2ab\sigma'_e + 2bl\sigma - \psi abl\Delta f$ and $E_1 = (1-\psi)abl\Delta f$ still hold with $0 \leq \psi \leq 1$ and $0 \leq \ell' \leq \ell$.

At this point, a simple change of variable is introduced for convenience. Define $\lambda = 1-\xi$ with $0 \leq \lambda \leq 1$.

Now observe that although the free energy of fusion is $abl\Delta f$ when $\Delta\phi_1$ is positive or negative, the free energy of fusion which can be apportioned is $abl\Delta f$ when $\Delta\phi_1$ is positive but is $(2ab\sigma'_e + 2bl\sigma)$ when $\Delta\phi_1$ is negative. Also, the free energy of fusion that is in fact apportioned is $\psi abl\Delta f$ when $\Delta\phi_1$ is positive, but is $\lambda(2ab\sigma'_e + 2bl\sigma)$ when $\Delta\phi_1$ is negative. Clearly then, the fraction of the free energy of fusion which can be apportioned that is apportioned is ψ when $\Delta\phi_1$ is positive, but is λ when $\Delta\phi_1$ is negative. If we always choose the same value for λ and ψ , then over the whole range of values for $\Delta\phi_1$, the fraction of the free energy of fusion which can be apportioned, has the same value. Let γ denote any particular value which is chosen for both ψ and λ , where $0 \leq \gamma \leq 1$.

Note that equal values of ψ and λ do not imply the same value of l' (except when $\Delta\phi_1 = 0$ as will become evident); as usual $\psi = \frac{l'}{l}$, but an expression for λ in terms of l' or vice versa remains to be obtained. In our approach, then, l' depends at least on the sign of $\Delta\phi_1$, and yet we utilize only one parameter, γ --the fraction of the free energy of fusion which can be apportioned that is apportioned--which is a constant over the whole range of values for $\Delta\phi_1$.

In summary, the barriers in terms of the apportionment parameter γ are

$$\left. \begin{aligned} \Delta\phi_1 + E_1 &= (1-\gamma)(2ab\sigma'_e + 2bl\sigma) \\ E_1 &= abl\Delta f - \gamma(2ab\sigma'_e + 2bl\sigma) \end{aligned} \right\} \text{ for } \Delta\phi_1 \leq 0$$

$$\left. \begin{aligned} \Delta\phi_1 + E_1 &= 2ab\sigma'_e + 2bl\sigma - \gamma abl\Delta f \\ E_1 &= (1-\gamma)abl\Delta f \end{aligned} \right\} \text{ for } \Delta\phi_1 \geq 0$$

where we now observe that $(1-\gamma)(2ab\sigma'_e + 2bl\sigma) = 2ab\sigma'_e + 2bl\sigma - \gamma abl\Delta f$ when $\Delta\phi_1 = 0$, i.e. $\Delta\phi_1 + E_1$ is a continuous function of l and Δf at the points $(l, \Delta f)$ for which $\Delta\phi_1 = 0$. Note that the greater the value of the apportionment parameter γ , the smaller the value of both $\Delta\phi_1 + E_1$ and E_1 .

An expression for l' is not needed in order to evaluate $S_{\text{Total}}(T)$ and $l(T)$. However, an expression for l' in terms of λ and vice versa will be derived in order to see how l' depends on other quantities in our model. Given $\Delta\phi_1 + E_1 = (1-\lambda)(2ab\sigma'_e + 2bl\sigma)$ for $\Delta\phi_1 < 0$, one can first find ψ when $\Delta\phi_1 < 0$ holds in terms of λ by equating the expressions

$$(1-\lambda)(2ab\sigma'_e + 2bl\sigma) = 2ab\sigma'_e + 2bl\sigma - \psi abl\Delta f$$

whence

$$\psi = \lambda \left(\frac{2ab\sigma'_e + 2bl\sigma}{abl\Delta f} \right)$$

or

$$\psi = \lambda \left(\frac{2\sigma'_e}{\ell\Delta f} + \frac{2\sigma}{a\Delta f} \right).$$

Clearly, equating these expressions and expressing ψ when $\Delta\phi_1 < 0$ in terms of λ is valid since decreasing $2ab\sigma'_e + 2b\ell\sigma$ by an amount $\psi ab\ell\Delta f$ must be equivalent to decreasing $2ab\sigma'_e + 2b\ell\sigma$ by $\lambda(2ab\sigma'_e + 2b\ell\sigma)$. Note that the expression $\left(\frac{2\sigma'_e}{\ell\Delta f} + \frac{2\sigma}{a\Delta f} \right)$ is always less than one when $\Delta\phi_1$ is negative. To see this, simply observe that $\Delta\phi_1 < 0$ implies $2ab\sigma'_e + 2b\ell\sigma < ab\ell\Delta f$, and then divide both sides of this inequality by $ab\ell\Delta f$. But $\psi = \frac{\ell'}{\ell}$ for all values of $\Delta\phi_1$ so that

$$\ell' = \lambda \ell \left(\frac{2\sigma'_e}{\ell\Delta f} + \frac{2\sigma}{a\Delta f} \right).$$

Note that since λ cannot exceed one, the largest possible value of ℓ' , i.e. the upper limit on ℓ' , is $\ell \left(\frac{2\sigma'_e}{\ell\Delta f} + \frac{2\sigma}{a\Delta f} \right)$ for $\Delta\phi_1 < 0$; as mentioned previously, this upper limit is indeed less than ℓ for $\Delta\phi_1 < 0$.

For completeness, one can also find λ when $\Delta\phi_1 > 0$ holds in terms of ψ by equating the expressions

$$(1-\lambda)(2ab\sigma'_e + 2b\ell\sigma) = 2ab\sigma'_e + 2b\ell\sigma - \psi ab\ell\Delta f$$

whence

$$\lambda = \frac{\psi}{\left(\frac{2\sigma'_e}{\ell\Delta f} + \frac{2\sigma}{a\Delta f} \right)}.$$

Clearly, equating these expressions and expressing λ when $\Delta\phi_1 > 0$ in terms of ψ is valid since decreasing $2ab\sigma'_e + 2b\ell\sigma$ by an amount $\psi ab\ell\Delta f$ must be equivalent to decreasing $2ab\sigma'_e + 2b\ell\sigma$ by $\lambda(2ab\sigma'_e + 2b\ell\sigma)$. Here again, $\psi = \frac{\ell'}{\ell}$, and $\lambda = \frac{\ell'}{\ell} \left(\frac{1}{\frac{2\sigma'_e}{\ell\Delta f} + \frac{2\sigma}{a\Delta f}} \right)$. Note that $\left(\frac{2\sigma'_e}{\ell\Delta f} + \frac{2\sigma}{a\Delta f} \right)$ is always greater than one when $\Delta\phi_1$ is positive.

In summary, then, for $\Delta\phi_1 \leq 0$, one chooses a value from zero to one for the parameter γ , whence $\lambda = \gamma$, and then calculates $\psi = \lambda \left(\frac{2\sigma'_e}{\ell\Delta f} + \frac{2\sigma}{a\Delta f} \right)$. For $\Delta\phi_1 \geq 0$, one chooses a value from zero to one for the parameter γ , whence $\psi = \gamma$, and then calculates $\lambda = \frac{\psi}{\left(\frac{2\sigma'_e}{\ell\Delta f} + \frac{2\sigma}{a\Delta f} \right)}$. Thus,

$$\left. \begin{aligned} \lambda &= \gamma \\ \psi &= \lambda \left(\frac{2\sigma'_e}{l\Delta f} + \frac{2\sigma}{a\Delta f} \right) \end{aligned} \right\} \text{ for } \Delta\phi_1 \leq 0$$

$$\left. \begin{aligned} \psi &= \gamma \\ \lambda &= \frac{\psi}{\left(\frac{2\sigma'_e}{l\Delta f} + \frac{2\sigma}{a\Delta f} \right)} \end{aligned} \right\} \text{ for } \Delta\phi_1 \geq 0$$

And, for all $\Delta\phi_1$, one can calculate l' from $l' = \psi l$ or from $l' = \lambda l \left(\frac{2\sigma'_e}{l\Delta f} + \frac{2\sigma}{a\Delta f} \right)$.

Incidentally, the constraint $2ab\sigma'_e + 2bl\sigma - \psi abl\Delta f \geq 0$ combined with $0 \leq \psi \leq 1$ implies that the inequality

$$0 \leq \psi \leq \text{the smaller of } 1 \text{ and } \left(\frac{2\sigma'_e}{l\Delta f} + \frac{2\sigma}{a\Delta f} \right)$$

must be satisfied, and clearly our theory has satisfied it.

Similarly, the constraint $abl\Delta f - \lambda(2ab\sigma'_e + 2bl\sigma) \geq 0$ combined with $0 \leq \lambda \leq 1$ implies that the inequality

$$0 \leq \lambda \leq \text{the smaller of } 1 \text{ and } \frac{1}{\left(\frac{2\sigma'_e}{l\Delta f} + \frac{2\sigma}{a\Delta f} \right)}$$

must be satisfied, and clearly our theory has satisfied it.

The approach developed above can readily be applied to incorporate into the model the constraint that E_2 be nonnegative. Here, $E_2 = 2ab\sigma_e - \psi abl\Delta f$ can be negative when E is positive, and E is always positive (except when $l = 2\sigma_e/\Delta f$, which gives $E = 0$). The requirement $E_2 \geq 0$ implies that one is not allowed to apportion all of the free energy of fusion $abl\Delta f$. If the amount $\psi abl\Delta f$ which is apportioned were to exceed $2ab\sigma_e$, then E_2 would be negative. Therefore, one has $E_2 = \eta 2ab\sigma_e$ where η is an apportionment parameter with $0 \leq \eta \leq 1$. And $E + E_2 = -2ab\sigma_e + abl\Delta f + \eta 2ab\sigma_e = abl\Delta f - (1-\eta)2ab\sigma_e$. For

convenience, make the change of variable $\theta = 1 - \eta$ with $0 \leq \theta \leq 1$ so that for all l and Δf

$$E_2 = (1 - \theta)2ab\sigma_e \quad \text{and} \quad E + E_2 = abl\Delta f - \theta 2ab\sigma_e.$$

Observe that the barrier $E + E_2$ to the destruction of the second and each subsequent stem cannot be smaller than the free energy increase E that occurs upon its destruction, which implies that an adsorbed second or subsequent stem cannot completely crystallize before the barrier to the formation of that stem is surmounted, i.e. that the upper limit, determined below, on l'' is less than l .

To find an expression for l'' in terms of θ , one first finds ψ in terms of θ by equating the expressions for E_2 , i.e.

$$(1 - \theta)2ab\sigma_e = 2ab\sigma_e - \psi abl\Delta f$$

whence

$$\psi = \theta \frac{2\sigma_e}{l\Delta f}.$$

Clearly, equating these expressions and expressing ψ in terms of θ is valid since decreasing $2ab\sigma_e$ by an amount $\psi abl\Delta f$ must be equivalent to decreasing $2ab\sigma_e$ by $\theta 2ab\sigma_e$. Note that the constraint $2ab\sigma_e - \psi abl\Delta f \geq 0$ implies that the inequality $0 \leq \psi \leq \frac{2\sigma_e}{l\Delta f}$ must be satisfied; since $0 \leq \theta \leq 1$ holds, we have indeed satisfied this inequality. Also note that $\frac{2\sigma_e}{l\Delta f}$ is always less than or equal to one since $l \geq \frac{2\sigma_e}{\Delta f}$ has been established. (Incidentally, $2ab\sigma_e - \psi abl\Delta f \geq 0$ does not imply constraints $l \leq \frac{2\sigma_e}{\psi \Delta f}$, $\Delta f \leq \frac{2\sigma_e}{\psi l}$, or $\sigma_e \geq \frac{\psi l \Delta f}{2}$.) Finally, recalling that $\psi = \frac{l''}{l}$ and substituting above gives $l'' = \theta \frac{2\sigma_e}{\Delta f}$.

In the special case $\gamma = \theta = 0$, our model reduces to the case $\psi = \psi = 0$ of the LH model which permits negative barriers for nonzero ψ .

VI. DETERMINATION OF THE SIGN OF $\Delta\phi_1$

At this point, one needs to determine when $\Delta\phi_1$ is positive, zero, and negative. Now $\Delta\phi_1 = 2ab\sigma'_e + 2bl\sigma - abl\Delta f \geq 0$ implies $bl(2\sigma - a\Delta f) \geq -2ab\sigma'_e$; and there are three cases to consider.

Case (a): $2\sigma - a\Delta f > 0$ or $\Delta f < \frac{2\sigma}{a}$. Then the inequality $l > \frac{-2ab\sigma'_e}{b(2\sigma - a\Delta f)}$ is always satisfied since l is always greater than zero, and hence $\Delta\phi_1 > 0$ holds.

Case (b): $2\sigma - a\Delta f = 0$ or $\Delta f = \frac{2\sigma}{a}$. Then $\Delta\phi_1 = 2ab\sigma'_e$, which is always positive or zero depending on σ'_e .

Thus, combining cases (a) and (b), we have $\Delta\phi_1 \geq 0$ for all l when $\Delta f \leq \frac{2\sigma}{a}$, where $\Delta\phi_1 = 0$ when both $\sigma'_e = 0$ and $\Delta f = \frac{2\sigma}{a}$.

Case (c): $2\sigma - a\Delta f < 0$ or $\Delta f > \frac{2\sigma}{a}$. Then $\Delta\phi_1 \geq 0$ implies $-bl(a\Delta f - 2\sigma) \geq$

$-2ab\sigma'_e$ or $l \leq \frac{\frac{2\sigma'_e}{\Delta f}}{1 - \frac{2\sigma}{a\Delta f}} = l_0$. Thus, when $\Delta f > \frac{2\sigma}{a}$, $\Delta\phi_1 \geq 0$ holds for $l \leq l_0$, and

$\Delta\phi_1 \leq 0$ holds for $l \geq l_0$. (Observe that as $\Delta f \rightarrow \frac{2\sigma}{a}$ from values greater than $\frac{2\sigma}{a}$, $l_0 \rightarrow \infty$.) There is, however, one further condition to consider here.

Recall that $l \geq \frac{2\sigma_e}{\Delta f}$ has been established. If $l_0 < \frac{2\sigma_e}{\Delta f}$ holds, then $l > l_0$ holds and consequently $\Delta\phi_1 < 0$ would hold for all l . To determine when $l_0 <$

$\frac{2\sigma_e}{\Delta f}$ holds, simply write $\frac{\frac{2\sigma'_e}{\Delta f}}{1 - \frac{2\sigma}{a\Delta f}} < \frac{2\sigma_e}{\Delta f}$, and noting that $\frac{2\sigma}{a\Delta f} < 1$, rearrange this

inequality to get $\frac{2\sigma}{a\Delta f} < \frac{\sigma_e - \sigma'_e}{\sigma_e}$. Now, if $\sigma_e \leq \sigma'_e$, this inequality would be $\frac{2\sigma}{a\Delta f} < 0$, which is never satisfied; hence $l_0 < \frac{2\sigma_e}{\Delta f}$ never occurs when $\sigma_e \leq \sigma'_e$. If

$\sigma_e > \sigma'_e$, $l_0 < \frac{2\sigma_e}{\Delta f}$ occurs when $\Delta f > \frac{2\sigma}{a} \left(\frac{\sigma_e}{\sigma_e - \sigma'_e} \right)$. Thus, if $\sigma_e > \sigma'_e$ and $\frac{2\sigma}{a} < \Delta f \leq \frac{2\sigma}{a} \left(\frac{\sigma_e}{\sigma_e - \sigma'_e} \right)$, $\Delta\phi_1 \geq 0$ holds for $l \leq l_0$ and $\Delta\phi_1 \leq 0$ holds for $l \geq l_0$, but for $\Delta f > \frac{2\sigma}{a} \left(\frac{\sigma_e}{\sigma_e - \sigma'_e} \right)$, $\Delta\phi_1 < 0$ holds for all l .

VII. EXPRESSIONS FOR S_{Total} (T) AND $l(T)$

If $\sigma_e \leq \sigma'_e$, our model with no negative barriers has

- (1) $\Delta\phi_1 + E_1 = 2ab\sigma'_e + 2bl\sigma - \gamma abl\Delta f$ for $\Delta f \leq \frac{2\sigma}{a}$
- (2) $\Delta\phi_1 + E_1 = 2ab\sigma'_e + 2bl\sigma - \gamma abl\Delta f$ for $\Delta f > \frac{2\sigma}{a}$ and $l \leq l_0$
- (2) $\Delta\phi_1 + E_1 = (1-\gamma)(2ab\sigma'_e + 2bl\sigma)$ for $\Delta f > \frac{2\sigma}{a}$ and $l \geq l_0$

and if $\sigma_e > \sigma'_e$,

- (1) $\Delta\phi_1 + E_1 = 2ab\sigma'_e + 2bl\sigma - \gamma abl\Delta f$ for $\Delta f \leq \frac{2\sigma}{a}$
- (2) $\Delta\phi_1 + E_1 = 2ab\sigma'_e + 2bl\sigma - \gamma abl\Delta f$ for $\frac{2\sigma}{a} < \Delta f \leq \frac{2\sigma}{a} \left(\frac{\sigma_e}{\sigma_e - \sigma'_e} \right)$ and $l \leq l_0$
- (2) $\Delta\phi_1 + E_1 = (1-\gamma)(2ab\sigma'_e + 2bl\sigma)$ for $\frac{2\sigma}{a} < \Delta f \leq \frac{2\sigma}{a} \left(\frac{\sigma_e}{\sigma_e - \sigma'_e} \right)$ and $l \geq l_0$
- (3) $\Delta\phi_1 + E_1 = (1-\gamma)(2ab\sigma'_e + 2bl\sigma)$ for $\Delta f > \frac{2\sigma}{a} \left(\frac{\sigma_e}{\sigma_e - \sigma'_e} \right)$.

The purpose of categories (1), (2), and (3) will be seen shortly.

When $\Delta\phi_1 + E_1 = 2ab\sigma'_e + 2bl\sigma - \gamma abl\Delta f$, $E_1 = (1-\gamma)abl\Delta f$, which we call Case I.

When $\Delta\phi_1 + E_1 = (1-\gamma)(2ab\sigma'_e + 2bl\sigma)$, $E_1 = abl\Delta f - \gamma(2ab\sigma'_e + 2bl\sigma)$, which we call Case II.

One always has

$$E_2 = (1-\theta)2ab\sigma_e$$

$$E + E_2 = -2ab\sigma_e + abl\Delta f + E_2 = abl\Delta f - \theta 2ab\sigma_e.$$

Also,

$$S(\ell, T) = \frac{N_0 A_0 (1 - \frac{B}{A})}{1 - \frac{B}{A} + \frac{B_1}{A}}$$

where $\frac{B}{A} = e^{-E/kT}$, $\frac{B_1}{A} = e^{-(E_1 - E_2)/kT}$, and $A_0 = \beta e^{-(\Delta\phi_1 + E_1)/kT}$.

Abbreviate $c' = \frac{2ab\sigma'_e}{kT}$, $c = \frac{2ab\sigma_e}{kT}$, $\alpha = \frac{2\sigma}{a\Delta f}$, and recall $\ell_1 = \frac{2\sigma_e}{\Delta f}$. Then $\frac{c}{\ell_1} = \frac{ab\Delta f}{kT}$, $\frac{\alpha c}{\ell_1} = \frac{2b\sigma}{kT}$, and $\frac{E}{kT} = -c + \frac{c}{\ell_1} \ell$. For Case I,

$$\frac{\Delta\phi_1 + E_1}{kT} = \frac{2ab\sigma'_e}{kT} + \frac{2bl\sigma}{kT} - \frac{\gamma ab\Delta f}{kT} = c' + \frac{c}{\ell_1} (\alpha - \gamma) \ell$$

$$\frac{E_1 - E_2}{kT} = \frac{(1-\gamma)ab\Delta f}{kT} - \frac{(1-\theta)2ab\sigma_e}{kT} = \frac{c}{\ell_1} (1-\gamma) \ell - (1-\theta)c$$

For Case II,

$$\frac{\Delta\phi_1 + E_1}{kT} = \frac{(1-\gamma)(2ab\sigma'_e + 2bl\sigma)}{kT} = (1-\gamma)c' + \frac{\alpha c}{\ell_1} (1-\gamma) \ell$$

$$\frac{E_1 - E_2}{kT} = \frac{abl\Delta f - \gamma(2ab\sigma'_e + 2bl\sigma)}{kT} - \frac{(1-\theta)2ab\sigma_e}{kT} = \frac{c}{\ell_1} (1-\alpha\gamma) \ell - \gamma c' - (1-\theta)c$$

For Case I,

$$S_I(\ell, T) = \frac{\beta N_0 e^{-c'} e^{-(\alpha-\gamma)c\ell/\ell_1} (1 - e^c e^{-c\ell/\ell_1})}{1 - e^c e^{-c\ell/\ell_1} + e^{(1-\theta)c} e^{-(1-\gamma)c\ell/\ell_1}}$$

For Case II,

$$S_{II}(\ell, T) = \frac{\beta N_0 e^{-(1-\gamma)c'} e^{-(1-\gamma)\alpha c\ell/\ell_1} (1 - e^c e^{-c\ell/\ell_1})}{1 - e^c e^{-c\ell/\ell_1} + e^{(1-\theta)c} e^{\gamma c'} e^{-(1-\alpha\gamma)c\ell/\ell_1}}$$

For any Δf in category (1), then,

$$S_{\text{Total}}^{(1)}(T) = \frac{1}{\ell_u} \int_{\ell_1}^{\infty} S_I(\ell, T) d\ell \quad \text{and} \quad \lambda^{(1)}(T) = \frac{\int_{\ell_1}^{\infty} \ell S_I(\ell, T) d\ell}{\int_{\ell_1}^{\infty} S_I(\ell, T) d\ell}$$

For any Δf in category (2),

$$S_{\text{Total}}^{(2)}(T) = \frac{1}{\ell_u} \int_{\ell_1}^{\ell_0} S_I(\ell, T) d\ell + \frac{1}{\ell_u} \int_{\ell_0}^{\infty} S_{II}(\ell, T) d\ell$$

and

$$\lambda^{(2)}(T) = \frac{\int_{\ell_1}^{\ell_0} \ell S_I(\ell, T) d\ell + \int_{\ell_0}^{\infty} \ell S_{II}(\ell, T) d\ell}{\int_{\ell_1}^{\ell_0} S_I(\ell, T) d\ell + \int_{\ell_0}^{\infty} S_{II}(\ell, T) d\ell}$$

For any Δf in category (3),

$$S_{\text{Total}}^{(3)}(T) = \frac{1}{\ell_u} \int_{\ell_1}^{\infty} S_{II}(\ell, T) d\ell \quad \text{and} \quad \lambda^{(3)}(T) = \frac{\int_{\ell_1}^{\infty} \ell S_{II}(\ell, T) d\ell}{\int_{\ell_1}^{\infty} S_{II}(\ell, T) d\ell}$$

For purposes of comparison, the LH model which permits negative barriers has, for all ℓ and Δf ,

$$\Delta\phi_1 + E_1 = 2ab\sigma'_e + 2b\ell\sigma - \psi ab\ell\Delta f \quad \text{and} \quad E_2 = 2ab\sigma_e - \psi ab\ell\Delta f$$

so that

$$\frac{E_1 - E_2}{kT} = (1 - \psi + \hat{\psi}) \frac{c}{\ell_1} \ell - c$$

and

$$S^{(\text{LH})}(\ell, T) = \frac{\beta N_0 e^{-c'} e^{-(\alpha - \psi)c\ell/\ell_1} (1 - e^c e^{-c\ell/\ell_1})}{1 - e^c e^{-c\ell/\ell_1} + e^c e^{-(1 - \psi + \hat{\psi})c\ell/\ell_1}}$$

and

$$S_{\text{Total}}^{(\text{LH})}(\ell, T) = \frac{1}{\ell_u} \int_{\ell_1}^{\infty} S^{(\text{LH})}(\ell, T) d\ell \quad \text{and} \quad \lambda^{(\text{LH})}(T) = \frac{\int_{\ell_1}^{\infty} \ell S^{(\text{LH})}(\ell, T) d\ell}{\int_{\ell_1}^{\infty} S^{(\text{LH})}(\ell, T) d\ell}$$

As is the case in the LH model, our model has two parameters. The most logical choice for θ is $\theta = \gamma$; however, even with $\theta = \gamma$, our integrals cannot be evaluated analytically. There seems to be no special case (other than $\theta =$

$\gamma = 0$) for which they could be evaluated analytically. At this point then, we proceed without setting $\theta = \gamma$.

VIII. EVALUATION OF THE $S_{\text{Total}}(T)$ AND $\lambda(T)$ --THE VARIABLE TRANSFORMATIONS FOR THE NUMERICAL INTEGRATIONS

The required numerical integrations were easily performed interactively on the VAX using the IMSL subroutine DQDAGS.¹⁰ Integrals to be evaluated using DQDAGS cannot have an infinite limit of integration. One way to proceed before using DQDAGS is to make a change of integration variable. Although DQDAGS can integrate functions with endpoints singularities (when the endpoints are finite), a change of variable which results in a transformed integrand which is bounded at all points including the finite endpoints in the new range of integration, is preferable to a change of variable which yields an improper integral albeit with finite integration limits. For each of the integrals appearing in $S_{\text{Total}}^{(1)}(T)$, $S_{\text{Total}}^{(2)}(T)$, and $S_{\text{Total}}^{(3)}(T)$, a variable transformation which resulted in a proper integral was in fact found. The same transformations did not transform the corresponding integrals in the numerators of $\lambda^{(1)}(T)$, $\lambda^{(2)}(T)$, and $\lambda^{(3)}(T)$ into proper integrals; however, the transformed integrands were of the form $(-\ln x)f(x)$ with the singularity resulting only from the factor $\ln x$ as $x \rightarrow 0$. This endpoint singularity could be handled by DQDAGS.

Consider first the integral in $S_{\text{Total}}^{(1)}(T)$. The variable transformation consists of defining

$$x = e^{(1-\gamma)c} e^{-(1-\gamma)c\ell/\ell_1}.$$

Note that $x(\ell \rightarrow \infty) = 0$; the constant $e^{(1-\gamma)c}$, i.e. the ℓ -independent factor, is chosen so that $x(\ell = \ell_1) = 1$. Solving for ℓ in terms

of x gives $\ell = \ell_1 \left[1 - \frac{\ln x}{(1-\gamma)c} \right]$ provided $\gamma \neq 1$. Then $d\ell = -\frac{\ell_1}{(1-\gamma)c} \left(\frac{1}{x} \right) dx$.

Furthermore, $e^{-(\alpha-\gamma)c\ell/\ell_1} = e^{-(\alpha-\gamma)c} x^{\frac{\alpha-\gamma}{1-\gamma}}$, $e^{-c\ell/\ell_1} = e^{-c} x^{\frac{1}{1-\gamma}}$, and

$e^{-(1-\gamma)c\ell/\ell_1} = e^{-(1-\gamma)c} x$ so that

$$S_{\text{Total}}^{(1)}(T) = \frac{\beta N_0}{\ell_u} \frac{e^{-c'} e^{-(\alpha-\gamma)c} \ell_1}{(1-\gamma)c} \int_0^1 \frac{x^{\frac{\alpha-\gamma}{1-\gamma}} (1-x)^{\frac{1}{1-\gamma}}}{1-x^{\frac{1}{1-\gamma}} + e^{(1-\theta)c} e^{-(1-\gamma)c} x} \left(\frac{1}{x}\right) dx$$

Simplifying gives

$$S_{\text{Total}}^{(1)}(T) = \frac{\beta N_0}{\ell_u} \frac{e^{-c'} e^{-(\alpha-\gamma)c} \ell_1}{(1-\gamma)c} \int_0^1 \frac{x^{\frac{\alpha-1}{1-\gamma}} (1-x)^{\frac{1}{1-\gamma}}}{1-x^{\frac{1}{1-\gamma}} + e^{-(\theta-\gamma)c} x} dx$$

This is one of the integrals that was evaluated numerically by DQDAGS.

Designate the integrand above as $f_1(x)$. Using the same variable

transformation to evaluate the numerator of $\ell^{(1)}(T)$ gives

$$\ell^{(1)}(T) = \frac{\int_0^1 \ell_1 \left[1 - \frac{\ln x}{(1-\gamma)c}\right] f_1(x) dx}{\int_0^1 f_1(x) dx} = \ell_1 + \frac{\ell_1}{(1-\gamma)c} \frac{\int_0^1 (-\ln x) f_1(x) dx}{\int_0^1 f_1(x) dx}$$

Next, using the same transformation on the integral $\int_{\ell_1}^{\ell_0} S_I(\ell, T) d\ell$ appearing in $S_{\text{Total}}^{(2)}(T)$ gives

$$\int_{\ell_1}^{\ell_0} S_I(\ell, T) d\ell = \beta N_0 \frac{e^{-c'} e^{-(\alpha-\gamma)c} \ell_1}{(1-\gamma)c} \int_{x_0}^1 f_1(x) dx$$

where

$$x_0 = x(\ell=\ell_0) = e^{(1-\gamma)c} e^{-(1-\gamma)c\ell_0/\ell_1} = e^{(1-\gamma)c} e^{-(1-\gamma)c'/(1-\alpha)}$$

with $\ell_0 = 2\sigma_e'/(1-\alpha)\Delta f$ as defined previously.

Similarly, the integral $\int_{\ell_1}^{\ell_0} \ell S_I(\ell, T) d\ell$ appearing in $\ell^{(2)}(T)$ becomes

$$\int_{\ell_1}^{\ell_0} \ell S_I(\ell, T) d\ell = \frac{\beta N_0 e^{-c'} e^{-(\alpha-\gamma)c} \ell_1}{(1-\gamma)c} \left\{ \ell_1 \int_{x_0}^1 f_1(x) dx + \frac{\ell_1}{(1-\gamma)c} \int_{x_0}^1 (-\ln x) f_1(x) dx \right\}$$

A different transformation is made on the integral $\int_{\ell_0}^{\infty} S_{II}(\ell, T) d\ell$ also appearing in $S_{\text{Total}}^{(2)}(T)$. Here, define

$$x = e^{(1-\gamma)(c-c')} e^{-(1-\gamma)\alpha c\ell/\ell_1}$$

Again $x(\ell \rightarrow \infty) = 0$; the constant $e^{(1-\gamma)(c-c')}$ is chosen so that $x(\ell=\ell_0) = x_0$, which is given above. Solving for ℓ gives $\ell = \frac{\ell_1}{\alpha c} \left[c - c' - \frac{\ln x}{(1-\gamma)} \right]$ provided $\gamma \neq 1$. Then $d\ell = -\frac{\ell_1}{(1-\gamma)\alpha c} \left(\frac{1}{x} \right) dx$. Furthermore, $e^{-(1-\gamma)\alpha c \ell / \ell_1} = e^{-(1-\gamma)(c-c') \ell_1 / x}$,

$$e^{-c\ell/\ell_1} = e^{-(c-c')/\alpha} x^{\frac{1}{(1-\gamma)\alpha}}, \text{ and } e^{-(1-\alpha\gamma)c\ell/\ell_1} = e^{\frac{-(c-c')(1-\alpha\gamma)}{\alpha}} x^{\frac{1-\alpha\gamma}{(1-\gamma)\alpha}}.$$

Substituting gives

$$\begin{aligned} \int_{\ell_0}^{\infty} S_{II}(\ell, T) d\ell &= \frac{\beta N_0 e^{-(1-\gamma)c'} e^{-(1-\gamma)(c-c')\ell_1}}{(1-\gamma)\alpha c} \\ &\cdot \int_0^{x_0} \frac{x \left[1 - e^c e^{-\left(\frac{c-c'}{\alpha}\right) x^{\frac{1}{(1-\gamma)\alpha}}} \right]}{1 - e^c e^{-\left(\frac{c-c'}{\alpha}\right) x^{\frac{1}{(1-\gamma)\alpha}}} + e^{(1-\theta)c} e^{\gamma c'} e^{-\left(\frac{c-c'}{\alpha}\right) (1-\alpha\gamma) x^{\frac{1-\alpha\gamma}{(1-\gamma)\alpha}}} } \left(\frac{1}{x} \right) dx \\ &= \frac{\beta N_0 e^{-(1-\gamma)c} \ell_1}{(1-\gamma)\alpha c} \int_0^{x_0} \frac{1 - e^c e^{-\left(\frac{c-c'}{\alpha}\right) x^{\frac{1}{(1-\gamma)\alpha}}} }{1 - e^c e^{-\left(\frac{c-c'}{\alpha}\right) x^{\frac{1}{(1-\gamma)\alpha}}} + e^{-(\theta-\gamma)c} e^c e^{-\left(\frac{c-c'}{\alpha}\right) x^{\frac{1-\alpha\gamma}{(1-\gamma)\alpha}}} } dx \end{aligned}$$

Designate the integrand above as $f_2(x)$. Similarly, the integral

$\int_{\ell_0}^{\infty} \ell S_{II}(\ell, T) d\ell$ appearing in $\ell^{(2)}(T)$ becomes

$$\int_{\ell_0}^{\infty} \ell S_{II}(\ell, T) d\ell = \frac{\beta N_0 e^{-(1-\gamma)c} \ell_1}{(1-\gamma)\alpha c} \left\{ \frac{(c-c')}{\alpha c} \ell_1 \int_0^{x_0} f_2(x) dx + \frac{\ell_1}{(1-\gamma)\alpha c} \int_0^{x_0} (-\ln x) f_2(x) dx \right\}$$

Thus,

$$S_{\text{Total}}^{(2)}(T) = \left(\frac{\beta N_0}{\ell_u} \frac{e^{-c'} e^{-(\alpha-\gamma)c} \ell_1}{(1-\gamma)c} \int_{x_0}^1 f_1(x) dx \right) + \left(\frac{\beta N_0}{\ell_u} \frac{e^{-(1-\gamma)c} \ell_1}{(1-\gamma)\alpha c} \int_0^{x_0} f_2(x) dx \right)$$

and

$$\lambda^{(2)}(T) = \frac{\left(\frac{1}{\beta N_0} \int_{\ell_1}^{\ell_0} \ell S_I(\ell, T) d\ell \right) + \left(\frac{1}{\beta N_0} \int_{\ell_0}^{\infty} \ell S_{II}(\ell, T) d\ell \right)}{\frac{\ell_u}{\beta N_0} S_{\text{Total}}^{(2)}(T)}$$

with the appropriate expressions for the integrals and $S_{\text{Total}}^{(2)}(T)$ to be substituted above.

Finally, consider the integral in $S_{\text{Total}}^{(3)}(T)$. The variable transformation to be made on this integral is

$$x = e^{(1-\gamma)\alpha c} e^{-(1-\gamma)\alpha c \ell / \ell_1}.$$

Again $x(\ell \rightarrow \infty) = 0$ and the constant $e^{(1-\gamma)\alpha c}$ is chosen so that $x(\ell = \ell_1) = 1$. Solving for ℓ gives $\ell = \ell_1 \left[1 - \frac{\ln x}{(1-\gamma)\alpha c} \right]$ provided $\gamma \neq 1$. Then $d\ell = -\frac{\ell_1}{(1-\gamma)\alpha c} \left(\frac{1}{x} \right) dx$. Furthermore, $e^{-(1-\gamma)\alpha c \ell / \ell_1} = e^{-(1-\gamma)\alpha c} x$, $e^{-c\ell / \ell_1} =$

$e^{-c} x^{\frac{1}{(1-\gamma)\alpha}}$, and $e^{-(1-\gamma)\alpha c \ell / \ell_1} = e^{-(1-\gamma)\alpha c} x^{\frac{1-\alpha\gamma}{(1-\gamma)\alpha}}$ so that

$$S_{\text{Total}}^{(3)}(T) = \frac{\beta N_0}{\ell_u} \frac{e^{-(1-\gamma)(c' + \alpha c)} \ell_1}{(1-\gamma)\alpha c} \int_0^1 \frac{\frac{1}{(1-x)^{\frac{1}{(1-\gamma)\alpha}}}}{1-x^{\frac{1}{(1-\gamma)\alpha}} + e^{-\theta c} e^{\gamma(c' + \alpha c)} x^{\frac{1-\alpha\gamma}{(1-\gamma)\alpha}}} dx$$

Designate the integrand above as $f_3(x)$. Using the same transformation to evaluate the numerator of $\lambda^{(3)}(T)$ gives

$$\lambda^{(3)}(T) = \ell_1 + \frac{\ell_1}{(1-\gamma)\alpha c} \frac{\int_0^1 (-\ln x) f_3(x) dx}{\int_0^1 f_3(x) dx}.$$

IX. RESULTS AND DISCUSSION

A VAX FORTRAN program was written to evaluate the required mathematical expressions. All calculations were done double precision using the model parameter values given in Figure 3 of Reference 4; namely, $a = b = 5 \times 10^{-8}$

cm, $\sigma = 10 \text{ erg/cm}^2$, $\sigma_e = 100 \text{ erg/cm}^2$, $T_m^\circ = 500 \text{ K}$, $\Delta h = 3 \times 10^9 \text{ ergs/cm}^3$, and $\Delta f = (T_m^\circ - T)\Delta h/T_m^\circ$, where Δh is the enthalpy of fusion at $T = T_m^\circ$. The average lamellar thickness calculated from the LH model is independent of σ'_e ; this is true for our model only for $\Delta f \leq \frac{2\sigma}{a}$, however. Other quantities such as $S_{\text{Total}}(T)$ do depend on σ'_e even in the LH model, and physically,¹¹ one expects $0 \leq \sigma'_e \leq \sigma_e$. In the case $\sigma'_e = 0$, our model is slightly simpler, for then

$$\left. \begin{aligned} \Delta\phi_1 + E_1 &= 2b\ell\sigma - \gamma ab\ell\Delta f \\ E_1 &= (1-\gamma)ab\ell\Delta f \end{aligned} \right\} \Delta f \leq \frac{2\sigma}{a}$$

$$\left. \begin{aligned} \Delta\phi_1 + E_1 &= (1-\gamma)2b\ell\sigma \\ E_1 &= ab\ell\Delta f - \gamma 2b\ell\sigma \end{aligned} \right\} \Delta f > \frac{2\sigma}{a}$$

Let us investigate our model in detail for the case $\sigma'_e = 0$ first; this is also the somewhat arbitrary choice for σ'_e made for the calculations^{1,2} for the LH model. For the values of a , σ , T_m° , and Δh given above, the temperature T^* for which $\Delta f = \frac{2\sigma}{a}$ is $T^* = 433\frac{1}{3}\text{K}$.

Given the parameter values above and now with the choice $\theta = \gamma$, the calculated average lamellar thickness vs. temperature curves (ℓ vs T) are plotted in Figure 1(a) for the selected values of $\gamma = 0$, $\frac{1}{4}$, and $\frac{1}{2}$. (Results for $\gamma > \frac{1}{2}$ will be discussed later.) Some of the data used to construct these plots is given in Table I. (For $\Delta f \leq \frac{2\sigma}{a}$, the average lamellar thickness is given by the expression for $\ell^{(1)}(T)$ given previously and for $\Delta f > \frac{2\sigma}{a}$, by the expression for $\ell^{(3)}(T)$ also given previously.) Clearly, ℓ decreases monotonically with decreasing T in agreement with typical experimental behavior. For most supercoolings, the magnitude of the ℓ values is of the order of 25-125Å, which is quite reasonable. Note that at least for all values of $\Delta f > \frac{2\sigma}{a}$, ℓ at a given T increases with increasing γ . Also, the numerical results shown in Figure 1(a) indicate that ℓ vs. T is relatively insensitive to the value of γ .

For comparison, we have reproduced part of Figure 3(b) of Reference 1 as our Figure 1(b), which shows the LH model λ vs. T curves with $\hat{\phi} = \psi$ for the selected values of $\psi = 0, \frac{1}{4}, \frac{1}{3},$ and $\frac{1}{2}$. Some of the data which we calculated in order to construct these plots is given in Table II. The LH model $\psi = 0$ curve is identical to our $\gamma = 0$ curve. For $\Delta f \leq \frac{2\sigma}{a}$, each of the LH model " ψ curves" is qualitatively similar but not quantitatively identical to its corresponding " γ curve" presented in Figure 1(a). Recall that the quantitative difference arises from the fact that the barrier E_2 has been constrained to be nonnegative, i.e. $E_2 = (1-\theta)2ab\sigma_e$. For $\Delta f > \frac{2\sigma}{a}$, however, the LH model ψ curves are in marked contrast to the γ curves; in particular, for each ψ curve, λ approaches infinity asymptotically as Δf approaches $\frac{2\sigma}{\psi a}$. This is the behavior which is known as the $\delta\lambda$ catastrophe.

One point is worth emphasizing here; namely the relationship between γ and ψ . In both our model and the LH model, $\psi = \frac{\ell'}{\ell}$, but this ratio in the LH model is a constant, whereas in our model

$$\psi = \begin{cases} \gamma \left(\frac{2\sigma'_e}{\ell\Delta f} + \frac{2\sigma}{a\Delta f} \right) & \Delta\phi_1 \leq 0 \\ \gamma & \Delta\phi_1 \geq 0 \end{cases}.$$

For the case $\sigma'_e = 0$, this becomes

$$\psi = \begin{cases} \gamma \frac{2\sigma}{a\Delta f} & \Delta f \geq \frac{2\sigma}{a} \\ \gamma & \Delta f \leq \frac{2\sigma}{a} \end{cases}.$$

Now, for any given ψ , say ψ_j , λ in the LH model is infinite for all $\Delta f \geq \frac{2\sigma}{\psi_j a}$; and for all $\Delta f \geq \frac{2\sigma}{\psi_j a}$, there is no finite value of λ for any $\psi \geq \psi_j$.

Equivalently, a value of $\psi \geq \psi_j$ is not possible for a chain-folded system for all $\Delta f \geq \frac{2\sigma}{\psi_j a}$, that is, high values of ψ do not lead to chain-folded polymer crystals at high enough supercooling according to the LH model. Experiment,

however, gives chain-folded crystals at high supercooling with an average lamellar thickness that decreases monotonically with decreasing temperature. As we have seen, our one-parameter (i.e. γ) model with $\sigma'_e = 0$ does reproduce this high supercooling behavior. And yet, high values of ψ , i.e. of the ratio $\frac{l'}{l}$, are not associated with our high-supercooling chain-folded systems. To see this, first introduce the dimensionless quantity x , where $0 < x < 1$. Then for any $\Delta f = \frac{2\sigma}{xa}$, $\psi = \gamma \frac{2\sigma}{a\Delta f} = \gamma x$. Since γ cannot exceed one, ψ in our model cannot exceed x_j for any $\Delta f \geq \frac{2\sigma}{x_j a}$, where x_j is any given value of x . But this is exactly what was found for ψ in the LH model, i.e. that a value of ψ greater than or equal to ψ_j is not possible for any $\Delta f \geq \frac{2\sigma}{\psi_j a}$. Thus, for $\Delta f > \frac{2\sigma}{a}$, our model, through the imposition of the constraint that barriers be nonnegative, places exactly the same upper limit, $\frac{2\sigma}{a\Delta f}$, on our ψ that is predicted for ψ in the LH model. However, for $\Delta f > \frac{2\sigma}{a}$, our model, unlike the LH model, predicts l vs. T in qualitative agreement with experiment.

Thus, the selected calculations done for our model indicate that, for the case $\sigma'_e = 0$, our model does not exhibit an infinite average lamellar thickness. Most importantly, our model predicts l vs. T curves which are monotonically decreasing with decreasing T in agreement with experiment. That is, we have successfully extended the LH model to higher supercooling. Also, this success, coupled with the numerical results shown in Figure 1(a), significantly increases our confidence in using $\gamma = 0$ as a first approximation for mathematical convenience in practice.⁷ Finally, our results show that the δl catastrophe of the LH theory is related to the failure to exclude negative barriers and moreover that the LH approach to polymer crystallization is in itself valid for high supercooling--given that negative barriers are forbidden. Prior to this work, the LH approach had always been described as one which is invalid at high supercooling.

One set of results with $\theta \neq \gamma$ is presented in Table III. Here we see that for $\gamma = \frac{1}{2}$ and $\theta = 1$, the calculated $l(T)$ differ only slightly from the case with $\gamma = \frac{1}{2}$ and $\theta = \frac{1}{2}$.

Next, we investigated our model for $\sigma'_e \neq 0$. (Recall that λ for the LH model is independent of σ'_e and that our model is independent of σ'_e for $\Delta f \leq \frac{2\sigma}{a}$.) Using the same values for a , b , σ , σ_e , T_m^* , and Δh as above and again with $\theta = \gamma$, λ vs. T curves for $\sigma'_e = 0, 60, 100$, and 150 erg/cm^2 --each with $\gamma = \frac{1}{2}$ --are plotted together in Figure 2. Some of the $\sigma'_e \neq 0$ data used to construct these plots is given in Table IV (and the $\sigma'_e = 0$ data has been seen previously in Table I). From Figure 2, we see that λ decreases monotonically with decreasing T for $0 < \sigma'_e \leq \sigma_e$ as well as for $\sigma'_e = 0$ and that λ vs. T is relatively insensitive to the value of $\sigma'_e \leq \sigma_e$. Thus our conclusions made immediately above for the case $\sigma'_e = 0$ are valid when $0 < \sigma'_e \leq \sigma_e$. For $\sigma'_e = 150 \text{ erg/cm}^2$, there is a relative minimum in λ vs. T near $T = 405 \text{ K}$, and the curve passes through a small and "diffuse" relative maximum at a lower temperature. Recall that one expects $0 \leq \sigma'_e \leq \sigma_e$ so that with $\sigma_e = 100 \text{ erg/cm}^2$, $\sigma'_e = 150 \text{ erg/cm}^2$ may not be realistic but is examined in order to explore the model predictions as a function of σ'_e .

The relationship between γ and ψ with $\sigma'_e \neq 0$ is worth emphasizing at this point. In doing so, one difference between the cases $\sigma'_e = 0$ and $\sigma'_e \neq 0$ will be found; namely, ψ can exceed ψ_j for some $\Delta f \geq \frac{2\sigma}{\psi_j a}$ when $\sigma'_e \neq 0$. To reiterate, in both our model and the LH model, $\psi = \frac{\lambda'}{\lambda}$, but this ratio in the LH model is a constant, whereas in our model

$$\psi(\lambda, T) = \begin{cases} \gamma \left(\frac{2\sigma'_e}{\lambda \Delta f} + \frac{2\sigma}{a \Delta f} \right) & \Delta\phi_1(\lambda, T) \leq 0 \\ \gamma & \Delta\phi_1(\lambda, T) \geq 0 \end{cases}$$

where the notation $\psi(\lambda, T)$ and $\Delta\phi_1(\lambda, T)$ emphasizes here the dependence of ψ and $\Delta\phi_1$ on λ and T . (The T dependence, of course, enters through Δf .) Recalling the conditions which govern the sign of $\Delta\phi_1$ then gives, when $\sigma_e > \sigma'_e$

$$\psi(\lambda, T) = \begin{cases} \gamma \left(\frac{2\sigma'_e}{\lambda \Delta f} + \frac{2\sigma}{a \Delta f} \right) & \begin{cases} \text{for all } \lambda \text{ when } \Delta f > \frac{2\sigma}{a} \left(\frac{\sigma_e}{\sigma_e - \sigma'_e} \right) \\ \text{for } \lambda \geq \lambda_0 \text{ when } \frac{2\sigma}{a} < \Delta f \leq \frac{2\sigma}{a} \left(\frac{\sigma_e}{\sigma_e - \sigma'_e} \right) \end{cases} \\ \gamma & \begin{cases} \text{for } \lambda \leq \lambda_0 \text{ when } \frac{2\sigma}{a} < \Delta f \leq \frac{2\sigma}{a} \left(\frac{\sigma_e}{\sigma_e - \sigma'_e} \right) \\ \text{for all } \lambda \text{ when } \Delta f \leq \frac{2\sigma}{a} \end{cases} \end{cases}$$

and when $\sigma_e \leq \sigma'_e$

$$\psi(\lambda, T) = \begin{cases} \gamma \left(\frac{2\sigma'_e}{\lambda \Delta f} + \frac{2\sigma}{a \Delta f} \right) & \text{for } \lambda \geq \lambda_0 \text{ when } \Delta f > \frac{2\sigma}{a} \\ \gamma & \begin{cases} \text{for } \lambda \leq \lambda_0 \text{ when } \Delta f > \frac{2\sigma}{a} \\ \text{for all } \lambda \text{ when } \Delta f \leq \frac{2\sigma}{a} \end{cases} \end{cases}$$

where $\lambda_0 = \frac{\frac{2\sigma'_e}{\Delta f}}{1 - \frac{2\sigma}{a \Delta f}}$. Furthermore, on an λ vs. T curve, one has

$$\psi(\lambda, T) = \begin{cases} \gamma \left(\frac{2\sigma'_e}{\lambda \Delta f} + \frac{2\sigma}{a \Delta f} \right) & \Delta\phi_1(\lambda, T) \leq 0 \\ \gamma & \Delta\phi_1(\lambda, T) \geq 0 \end{cases}$$

where the conditions which govern the sign of $\Delta\phi_1(\lambda, T)$ are those given above for $\Delta\phi_1(\ell, T)$ but with ℓ replaced by λ . Therefore, the temperature T_0 of a point (λ_0, T_0) on an λ vs. T curve and at which $\Delta\phi_1(\lambda, T) = \Delta\phi_1(\lambda_0, T_0) = 0$ is the solution to the following non-linear algebraic equation in the one unknown T :

$$\lambda^{(2)}(T) = \lambda_0$$

or

$$\frac{\int_{\lambda_1}^{\lambda_0} \lambda S_I d\lambda + \int_{\lambda_0}^{\infty} \lambda S_{II} d\lambda}{\int_{\lambda_1}^{\lambda_0} S_I d\lambda + \int_{\lambda_0}^{\infty} S_{II} d\lambda} = \frac{\frac{2\sigma'_e}{\Delta f}}{1 - \frac{2\sigma}{a\Delta f}}$$

If $\sigma_e > \sigma'_e$, T_0 will correspond to a value of Δf in the range $\frac{2\sigma}{a} < \Delta f \leq \frac{2\sigma}{a} \left(\frac{\sigma_e}{\sigma_e - \sigma'_e} \right)$, but if $\sigma_e \leq \sigma'_e$, T_0 will correspond to a value of Δf in the range $\Delta f > \frac{2\sigma}{a}$.

Rather than attempt to solve the above equation iteratively, one simply plots the left-hand side $\lambda^{(2)}(T)$ vs. T and the right-hand side $\lambda_0(T)$ vs. T on the same graph, and T_0 is given by a point of intersection of the two curves. Note that as Δf approaches $\frac{2\sigma}{a}$ from values greater than $\frac{2\sigma}{a}$, λ_0 approaches infinity and that λ_0 decreases monotonically with decreasing T for $\Delta f > \frac{2\sigma}{a}$. For each of the λ vs. T curves with $\sigma'_e \neq 0$, we found one point of intersection (λ_0, T_0) , which is designated on each curve by an open circle. We also found that $\lambda^{(2)}(T) > \lambda_0$ holds when $T < T_0$ and that $\lambda^{(2)}(T) < \lambda_0$ holds when $T > T_0$. Thus, $\Delta\phi(\lambda, T) < 0$ holds for $T < T_0$ and $\Delta\phi(\lambda, T) > 0$ holds for $T > T_0$. Our final result is that, on an λ vs. T curve,

$$\psi = \begin{cases} \gamma \left(\frac{2\sigma'_e}{\lambda\Delta f} + \frac{2\sigma}{a\Delta f} \right) & 0 < T \leq T_0 \\ \gamma & T_0 \leq T < T_m^* \end{cases}$$

Note that if the dimensionless quantity x , $0 < x < 1$, is again introduced by writing $\Delta f = \frac{2\sigma}{xa}$, then $\psi = \gamma x \left(\frac{a\sigma'_e}{\lambda\sigma} + 1 \right)$ so that, unlike the case $\sigma'_e = 0$, ψ can exceed x_j for some $\Delta f \geq \frac{2\sigma}{x_j a}$, where x_j is any given value of x .

Now, upon proceeding to consider results for $\gamma > \frac{1}{2}$, our basic conclusions--especially the fact that we have removed the $\delta\lambda$ catastrophe at high supercooling--remain intact; however, we do not obtain λ vs. T curves which are monotonically decreasing for all T when γ is "sufficiently" large. Using the same values for a , b , σ , σ_e , T_m^* , and Δh as previously and again with $\theta = \gamma$ and $\sigma'_e = 0$, the calculated λ vs. T curves for the selected values of $\gamma = \frac{1}{2}$, $\frac{3}{4}$, .90, and .95 are plotted in Figure 3(a), and the curve for $\gamma =$

.99 appears in Figure 4. Some of the data used to construct these plots is given in Table V. The effect of γ on \bar{l} as a function of T is readily apparent. First, the curve for $\gamma = \frac{1}{2}$ appears on closer examination, to exhibit a discontinuity or break in its slope at the temperature $T^* = 433\frac{1}{3}K$ for which $\Delta f = \frac{2\sigma}{a}$. (This statement will be qualified later.) As for $\gamma = \frac{1}{2}$, \bar{l} for $\gamma = \frac{3}{4}, .9, .95$, and $.99$ does decrease with decreasing T for all T for which $\Delta f > \frac{2\sigma}{a}$, and there appears to be a break in the slope of \bar{l} vs. T at $T = T^*$. Unlike for $\gamma = \frac{1}{2}$, the higher γ curves pass through a relative minimum at a temperature for which $\Delta f < \frac{2\sigma}{a}$; the temperature T_* at which this minimum occurs increases with γ (for $\gamma = \frac{3}{4}$, it occurs between $T = 440$ and $433\frac{1}{3}K$ and so can hardly be seen on the plot.) Also, over the interval $T < T_*$, \bar{l} vs. T is at a relative maximum at $T = T^*$. Finally, note that \bar{l} vs. T curves for $.99 < \gamma < 1$ are qualitatively similar to the $\gamma = .99$ curve and do not exhibit an infinite average lamellar thickness. The numerical integrations in the expressions for $\bar{l}^{(1)}(T)$ and $\bar{l}^{(3)}(T)$ could not be done for $\gamma = 1$ as a result of the factor $(1-\gamma)$ appearing in various denominators.

For comparison, we have reproduced part of Figure 3(b) of Reference 1 as our Figure 3(b), which shows the LH model \bar{l} vs. T curves with $\hat{\psi} = \psi$ for the selected values of $\psi = \frac{1}{2}, \frac{3}{4}, .90$, and $.95$. Some of the data which we calculated in order to construct these plots is given in Table VI. These LH model ψ curves exhibit the δl catastrophe as Δf approaches $\frac{2\sigma}{\psi a}$, as do all LH curves for $.95 < \psi \leq 1$. The curves for $.95 < \psi \leq 1$ are similar to the $\psi = .95$ curve; since integrations can be done analytically in the LH model when $\hat{\psi} = \psi$, \bar{l} vs. T for $\psi = 1$ was able to be obtained.¹

Thus, for high enough γ , our $\sigma'_e = 0$ model \bar{l} vs. T curves appear to have a break in slope at $T = T^*$. We suspect that there is indeed a break in slope at $T = T^*$ because the relation

$$\psi = \begin{cases} \gamma \frac{2\sigma}{a\Delta f} & \Delta f \geq \frac{2\sigma}{a} \\ \gamma & \Delta f \leq \frac{2\sigma}{a} \end{cases}$$

implies that $\frac{d\lambda}{dT}$ is discontinuous at $\Delta f = \frac{2\sigma}{a}$; however, we have not evaluated $\frac{d\lambda}{dT}$ at $\Delta f = \frac{2\sigma}{a}$. The break in slope is apparently indiscernible up to γ values of about $\frac{1}{2}$, where the slope of λ vs. T has the same sign (positive) regardless of whether the point $\Delta f = \frac{2\sigma}{a}$ is approached from values of Δf higher or lower than $\frac{2\sigma}{a}$. As γ increases, however, the break becomes pronounced with the concomitant appearance of a relative maximum in λ at $T = T^*$ and a relative minimum in λ at $T = T_*$; necessarily then, the slope of λ vs. T as Δf approaches $\frac{2\sigma}{a}$ from values less than $\frac{2\sigma}{a}$ becomes negative. We will refer to this undesirable behavior, manifest at high values of γ , as the λ anomaly. Unlike the $\delta\lambda$ catastrophe in the LH model, the relative maximum in λ vs. T , as noted above, always appears at $\Delta f = \frac{2\sigma}{a}$ for all values of γ given that $\sigma'_e = 0$.

Next, we consider $\sigma'_e \neq 0$ for high values of γ . The λ vs. T curves for $\sigma'_e = 0, 60, 100$, and 150 ergs/cm^2 --each with $\gamma = \frac{3}{4}$ --are presented in Figure 5. The curves pass through a common relative minimum between $T = 440$ and $433\frac{1}{3} \text{ K}$ (for which $\Delta f < \frac{2\sigma}{a}$), and then each curve rises and passes through a relative maximum, that maximum being relatively higher and occurring at higher Δf the larger the value of σ'_e . At each maximum, there would appear to be a break in the slope of λ vs. T . Having passed through its maximum, each curve decreases monotonically with decreasing T thereafter.

One should be careful to note that what appears to be a break in the slope of λ vs. T when $\sigma'_e \neq 0$ is probably not a break in slope; $\frac{d\lambda^{(2)}(T)}{dT}$ should be continuous for all relevant T . Whether a break in the slope of λ vs. T occurs at $\Delta f = \frac{2\sigma}{a}$ when $\sigma'_e \neq 0$ as was presumed true for $\sigma'_e = 0$ cannot be determined conclusively from the appearance of the graphs, although the break appears to be absent.

Qualitatively similar λ vs. T curves are obtained for $\gamma = 0.9$ and $\sigma'_e = 0, 60, 100$ and 150 ergs/cm^2 as is shown in Figure 6. See also Table VII. The relative maxima are higher and "sharper" than the corresponding $\gamma = \frac{3}{4}$ curves, and they have moved to higher temperature. For $\gamma = 0.99$, the analogous

curves, shown in Figure 7, exhibit λ values which are unrealistically large as well as maxima which are extremely "sharp".

Thus, from the graphs, we see that the λ anomaly becomes more pronounced but moves to higher temperature as γ increases for a fixed nonzero value of σ'_e . That is, although the relative maximum in λ vs. T can appear at some $\Delta f > \frac{2\sigma}{a}$ when σ'_e is nonzero, the maximum becomes less pronounced as it moves to lower temperature upon a decrease in γ . Our model, then, does not fail at high supercooling, but does exhibit anomalous behavior for temperatures corresponding to values of Δf "just" greater and "just" less than $\frac{2\sigma}{a}$. This undesirable behavior is pronounced for large values of γ and is more pronounced for larger values of σ'_e for a given γ .

We can easily rationalize mathematically how our calculated λ vs. T curves can rise with decreasing T for some $\Delta f > \frac{2\sigma}{a}$ when σ'_e is nonzero. Recall that the expression for $\lambda^{(2)}(T)$, namely

$$\lambda^{(2)}(T) = \frac{\int_{\lambda_1}^{\lambda_0} \lambda S_I(\lambda, T) d\lambda + \int_{\lambda_0}^{\infty} \lambda S_{II}(\lambda, T) d\lambda}{\int_{\lambda_1}^{\lambda_0} S_I(\lambda, T) d\lambda + \int_{\lambda_0}^{\infty} S_{II}(\lambda, T) d\lambda}$$

contains two different integrands $S_I(\lambda, T)$ and $S_{II}(\lambda, T)$. Depending on σ'_e , γ , and T , the contribution of the integrals involving $S_I(\lambda, T)$ to $\lambda^{(2)}(T)$ may outweigh the contribution of the integrals involving $S_{II}(\lambda, T)$, and in some cases, our calculations show that to a very good approximation

$$\lambda^{(2)}(T) \approx \frac{\int_{\lambda_1}^{\lambda_0} \lambda S_I(\lambda, T) d\lambda}{\int_{\lambda_1}^{\lambda_0} S_I(\lambda, T) d\lambda} \quad \text{with } \lambda_0 \text{ approaching infinity.}$$

But this is our expression for $\lambda^{(1)}(T)$ for the interval $\Delta f \leq \frac{2\sigma}{a}$, and the results of our calculations using $\lambda^{(1)}(T)$ have been found to differ little from results using $\lambda^{(LH)}(T)$, i.e. the LH theory. Not unexpectedly then, $\lambda^{(2)}(T)$ can increase with decreasing T for some $\Delta f > \frac{2\sigma}{a}$. We note that the

numerator of $S_I(\ell, T)$, like the numerator of $S^{(LH)}(\ell, T)$, contains the factor $A_0 = e^{-c'} e^{-b\ell(2\sigma - \gamma a \Delta f)/kT}$, the form of which has been associated with¹⁰ increases in ℓ with decreasing T .

X. CONCLUSIONS

We have constructed a model of polymer crystallization which extends the LH theory by excluding negative free energy barriers, and we have shown that the $\delta\ell$ catastrophe of the LH theory is related to the failure to exclude these negative barriers. Our results show that the new model is more consistent with experimental behavior at very high supercooling.

Our results with $\sigma'_e = 0$ clearly indicate that the ℓ anomaly in our model--and in part the $\delta\ell$ catastrophe of the LH theory--are associated with the interval $\Delta f \leq \frac{2\sigma}{a}$ and are thus connected to the expression $\Delta\phi_1 + E_1 = 2ab\sigma'_e + 2b\ell\sigma - \gamma ab\ell\Delta f$. The ℓ anomaly also appears to be connected to this expression even when $\sigma'_e \neq 0$, i.e. even when the maximum in ℓ vs. T occurs at a temperature for which Δf exceeds $\frac{2\sigma}{a}$. Although high values of γ and ψ are considered unrealistic as has been elucidated⁶ recently, however, there is no guarantee that the LH theory as well as our extension of it has not failed to incorporate an as yet unknown constraint or feature which would improve the model results at high γ values. For example, high γ values may be unrealistic, but the ℓ values for high γ from an improved model may simply be unrealistically large but nevertheless monotonically decreasing with decreasing T for all T .

In conclusion, we hope to extend our modification of the LH approach to polymer crystallization to treat the interesting systems which interact with an applied electric field.

References

- (1) Scheinbeim, J.I.; Newman, B.A.; Sen, A. Macromolecules 1986, 19, 1454.
- (2) Marand, H.L.; Stein, R.S.; Stack, G.M. J. Polym. Sci. Polym. Phys. Ed. 1988, 26, 1361.
- (3) Marand, H.L.; Stein, R.S. J. Polym. Sci. Polym. Phys. Ed. 1989, 27, 1089.
- (4) Lauritzen, Jr., J.I.; Hoffman, J.D. J. Appl. Phys. 1973, 44, 4340.
- (5) Hoffman, J.D.; Davis, G.T.; Lauritzen, Jr., J.I. in Treatise on Solid State Chemistry; Vol. 3, Chapter 7, Plenum Press: New York, 1976.
- (6) Sanchez, I.C.; DiManzio, E.A. J. Chem. Phys. 1971, 55, 893.
- (7) Hoffman, J.D.; Miller, R.L. Macromolecules 1989, 22, 3038.
- (8) Frank, F.C.; Tosi, M. Proc. Roy. Soc. (London) 1961, A263, 323.
- (9) Turnbull, D.; Fisher, J.C. J. Chem. Phys. 1949, 17, 71.
- (10) User's Manual-Math/Library-Fortran Subroutines for Mathematical Applications; IMSL, Inc, 1987.
- (11) Hoffman, J.D.; Frolen, L.J.; Ross, G.S.; Lauritzen, Jr., J.I. Res. Nat. Bur. Stand. 1975, 79A, 671.
- (12) Sanchez, I.C. J. Macromol. Sci.-Revs. Macromol. Chem. 1974, C10, 113.

FIGURE CAPTIONS

- Figure 1(a). Plots of Average Lamellar Thickness (\AA) vs. Temperature (K) for $\gamma = 0, \frac{1}{4},$ and $\frac{1}{2}$, each with $\sigma'_e = 0$ and $\theta = \gamma$. See Section IX for $a, b, \sigma, \sigma_e, T_m^*$, and Δh which are the same for all of the figures. At $T = 433\frac{1}{3}$ K (i.e. $\Delta f = \frac{2\sigma}{a}$), $\Delta\phi_1 = 0$.
- For $T \geq 433\frac{1}{3}$ K, $\Delta\phi_1 \geq 0$ and $\psi = \gamma$ and $\lambda = \gamma \left(\frac{a\Delta f}{2\sigma} \right)$.
- For $T \leq 433\frac{1}{3}$ K, $\Delta\phi_1 \leq 0$ and $\psi = \gamma \left(\frac{2\sigma}{a\Delta f} \right)$ and $\lambda = \gamma$.
- Figure 1(b). Plots of Average Lamellar Thickness (\AA) vs. Temperature (K) for $\psi = 0, \frac{1}{4}, \frac{1}{3},$ and $\frac{1}{2}$, each with $\phi = \psi$, reproduced from the Lauritzen-Hoffman Model (Reference 1); plots are independent of σ'_e .
- Figure 2. Plots of Average Lamellar Thickness (\AA) vs. Temperature (K) for $\sigma'_e = 0, 60, 100,$ and 150 ergs/cm^2 , each with $\theta = \gamma = \frac{1}{2}$. Each open circle designates the point (λ_0, T_0) at which $\Delta\phi_1(\lambda, T) = 0$. For $T \geq T_0$, $\Delta\phi_1 \geq 0$, $\psi = \gamma$, and $\lambda = \gamma \left(\frac{ab\lambda\Delta f}{2ab\sigma'_e + 2b\lambda\sigma} \right)$. For $T \leq T_0$, $\Delta\phi_1 \leq 0$, $\psi = \gamma \left(\frac{2\sigma'_e}{\lambda\Delta f} + \frac{2\sigma}{a\Delta f} \right)$, and $\lambda = \gamma$.
- Figure 3(a). Plots of Average Lamellar Thickness (\AA) vs. Temperature (K) for $\gamma = \frac{1}{2}, \frac{3}{4}, 0.90,$ and 0.95 , each with $\sigma'_e = 0$ and $\theta = \gamma$. As in Figure 1(a), $\Delta\phi_1 = 0$ at $T = 433\frac{1}{3}$ K.
- Figure 3(b). Plots of Average Lamellar Thickness (\AA) vs. Temperature (K) for $\psi = \frac{1}{2}, \frac{3}{4}, .90,$ and $.95$, each with $\phi = \psi$, reproduced from the Lauritzen-Hoffman Model (Reference 1); plots are independent of σ'_e .
- Figure 4. Plots of Average Lamellar Thickness (\AA) vs. Temperature (K) for $\theta = \gamma = .99$ and $\sigma'_e = 0$. As in Figure 1(a), $\Delta\phi_1 = 0$ at $T = 433\frac{1}{3}$ K.

- Figure 5. Plots of Average Lamellar Thickness (\AA) vs. Temperature (K) for $\sigma'_e = 0, 60, 100, \text{ and } 150 \text{ ergs/cm}^2$, each with $\theta - \gamma = \frac{3}{4}$. As in Figure 2, each open circle identifies the temperature T_0 at which $\Delta\phi_1(\lambda, T) = 0$.
- Figure 6. Plots of Average Lamellar Thickness (\AA) vs. Temperature (K) for $\sigma'_e = 0, 60, 100, \text{ and } 150 \text{ ergs/cm}^2$, each with $\theta - \gamma = .90$. As in Figure 2, each open circle identifies the temperature T_0 at which $\Delta\phi_1(\lambda, T) = 0$.
- Figure 7. Plots of Average Lamellar Thickness (\AA) vs. Temperature (K) for $\sigma'_e = 0, 60, 100 \text{ and } 150 \text{ ergs/cm}^2$, each with $\theta - \gamma = .99$. For $\sigma'_e = 0, 60, 100, \text{ and } 150 \text{ ergs/cm}^2$, $T_0 = 433\frac{1}{3} \text{ K}, 432.2 \text{ K}, 432.1 \text{ K}, \text{ and } 432.0 \text{ K}$, respectively. As in Figure 2, T_0 is the temperature at which $\Delta\phi_1(\lambda, T) = 0$.

TABLE CAPTIONS

- Table I. Average Lamellar Thickness (\AA) as a function of Temperature (K) for $\gamma = 0$ and for $\gamma = \frac{1}{2}$, each with $\sigma'_e = 0$ and $\theta = \gamma$. See Figure 1(a). See Section IX for a , b , σ , σ_e , T_m° , and Δh , which are the same for all of the tables.
- Table II. Average Lamellar Thickness (\AA) as a function of Temperature (K) for $\psi = \frac{1}{2}$ with $\phi = \psi$, reproduced from the Lauritzen-Hoffman (LH) Model (Reference 4); data is independent of σ'_e . See Figure 1(b).
- Table III. Average Lamellar Thickness (\AA) as a function of Temperature (K) for $\gamma = \frac{1}{2}$, $\theta = 1$, and $\sigma'_e = 0$.
- Table IV. Average Lamellar Thickness (\AA) as a function of Temperature (K) for $\sigma'_e = 60, 100$, and 150 ergs/cm^2 , each with $\theta = \gamma = \frac{1}{2}$. See Figure 2.
- Table V. Average Lamellar Thickness (\AA) as a function of Temperature (K) for $\gamma = .90$ with $\sigma'_e = 0$ and $\theta = \gamma$. See Figure 3(a).
- Table VI. Average Lamellar Thickness (\AA) as a function of Temperature (K) for $\psi = .90$ with $\phi = \psi$, reproduced from the Lauritzen-Hoffman (LH) Model (Reference 4); data is independent of σ'_e . See Figure 3(b).
- Table VII. Average Lamellar Thickness (\AA) as a function of Temperature (K) for $\sigma'_e = 60, 100$, and 150 ergs/cm^2 , each with $\theta = \gamma = .90$. See Figure 6.

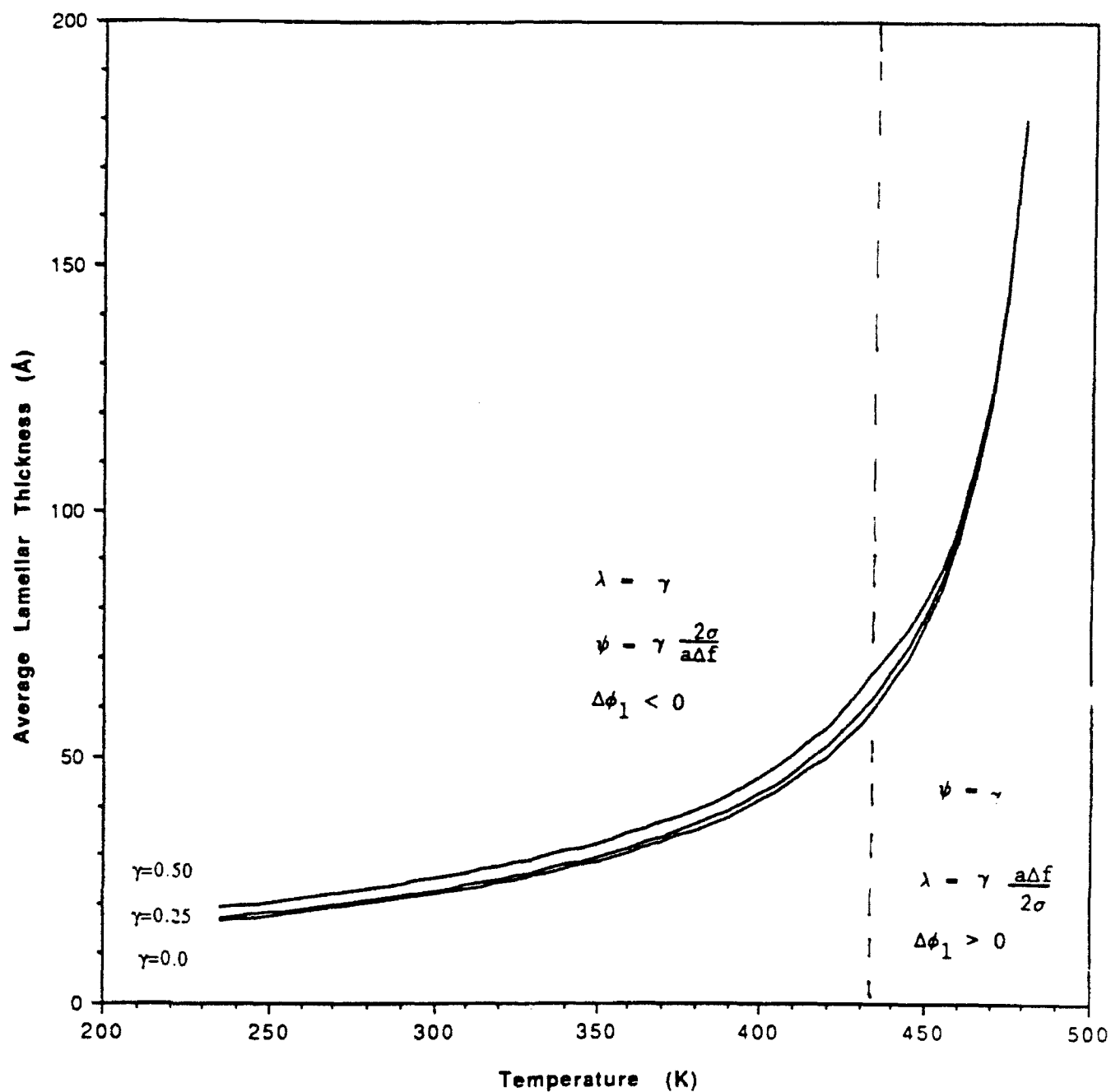


Figure 1(a).

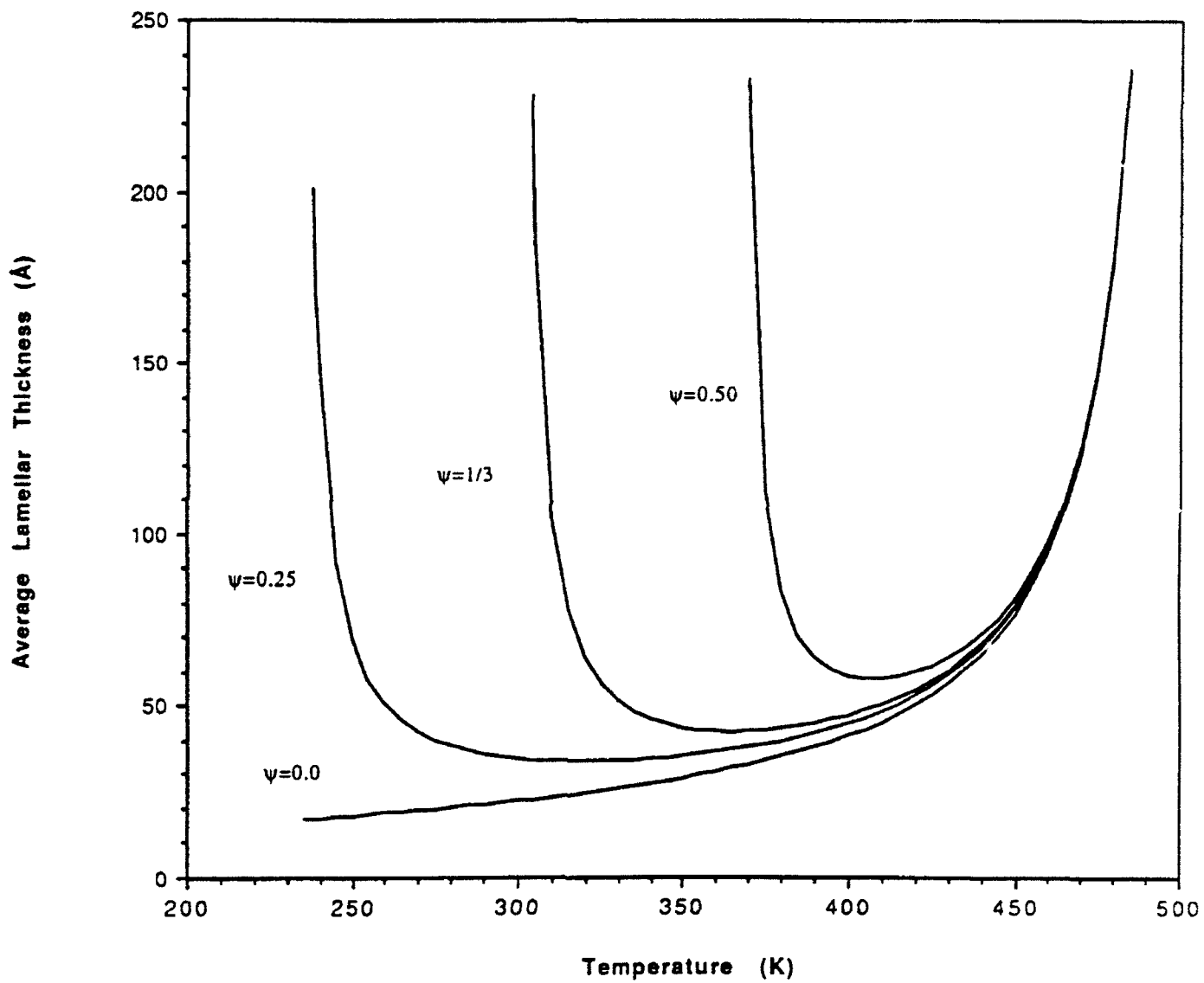


Figure 1(b).

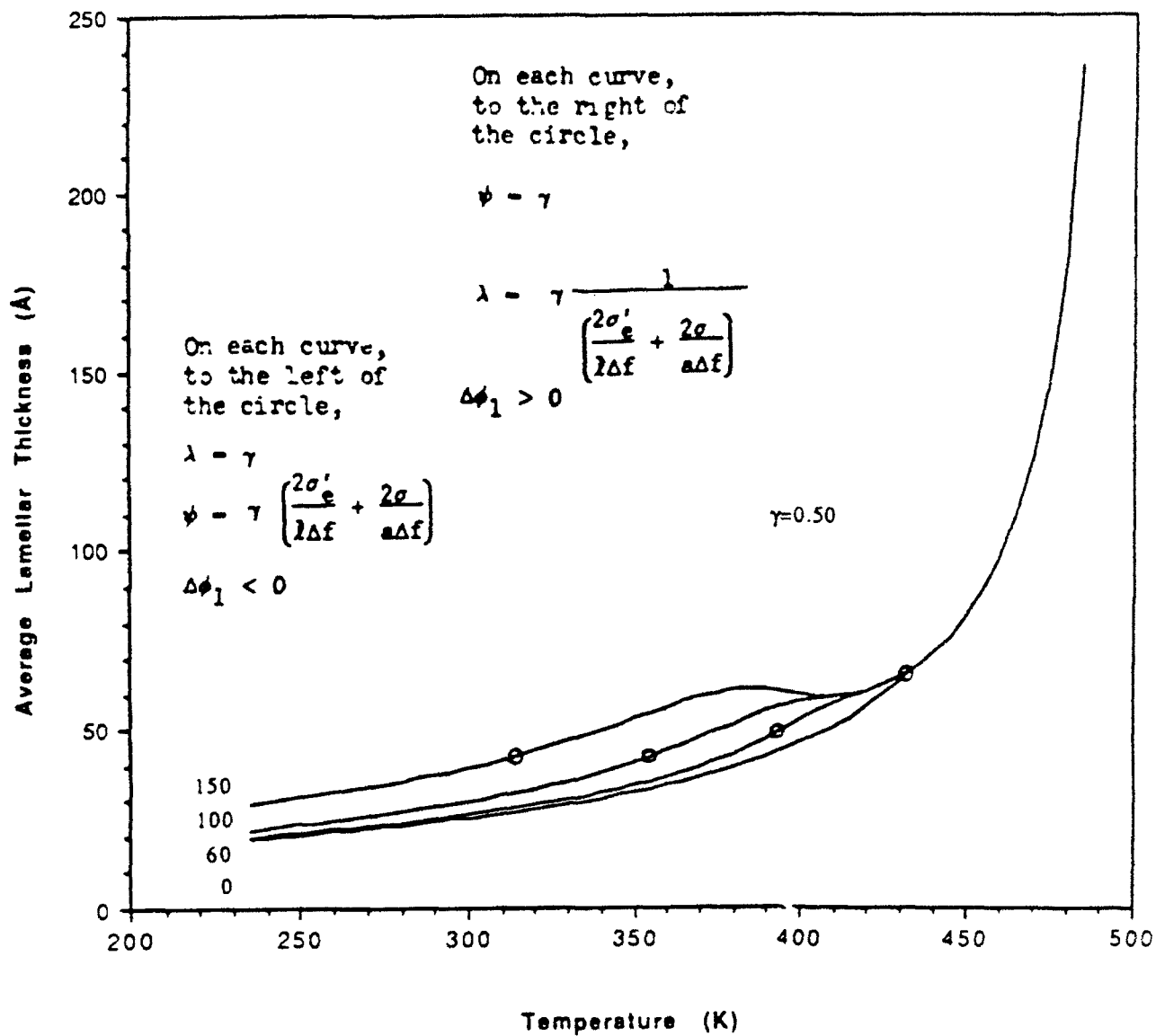


Figure 2.

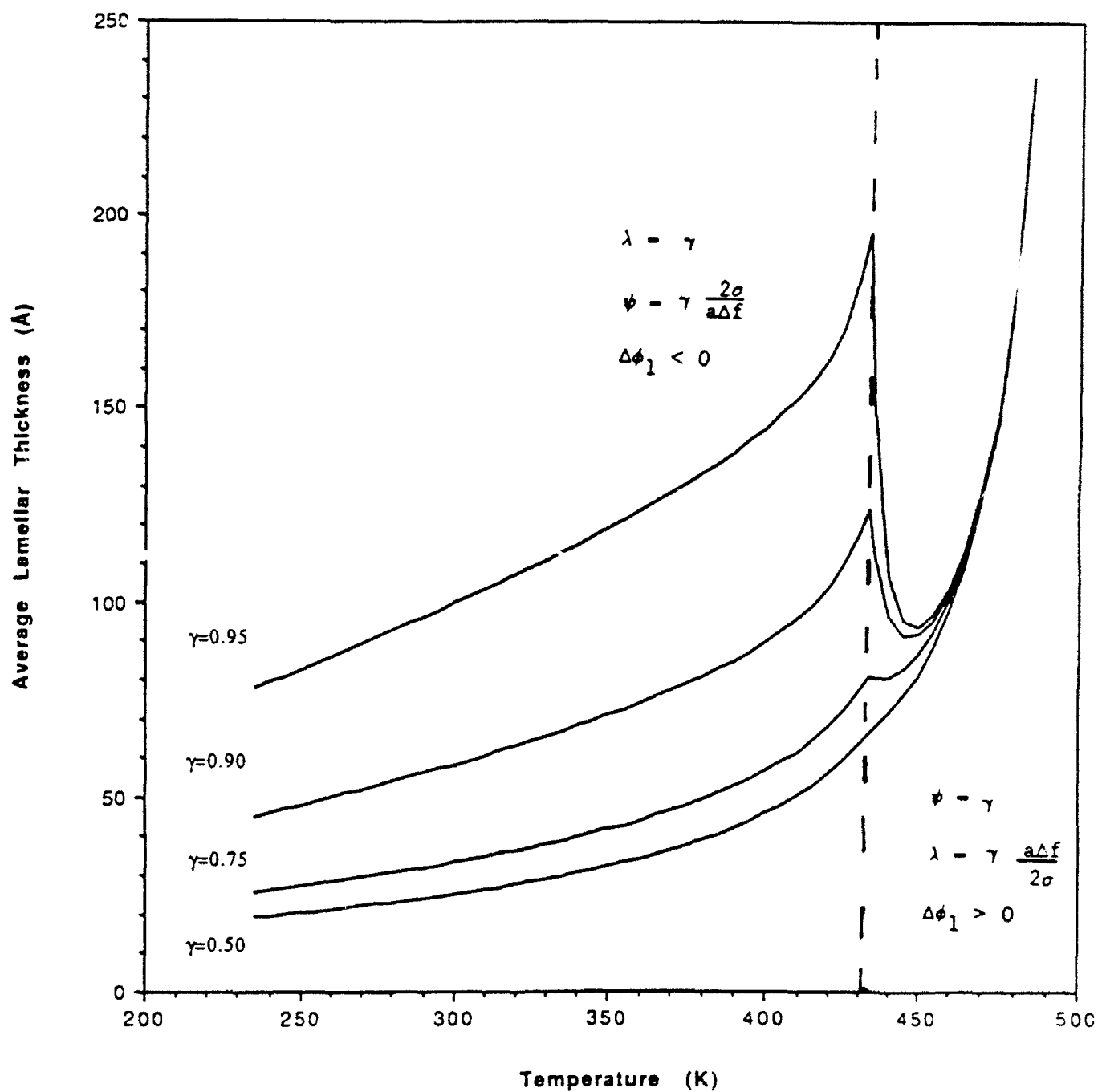


Figure 3(a).

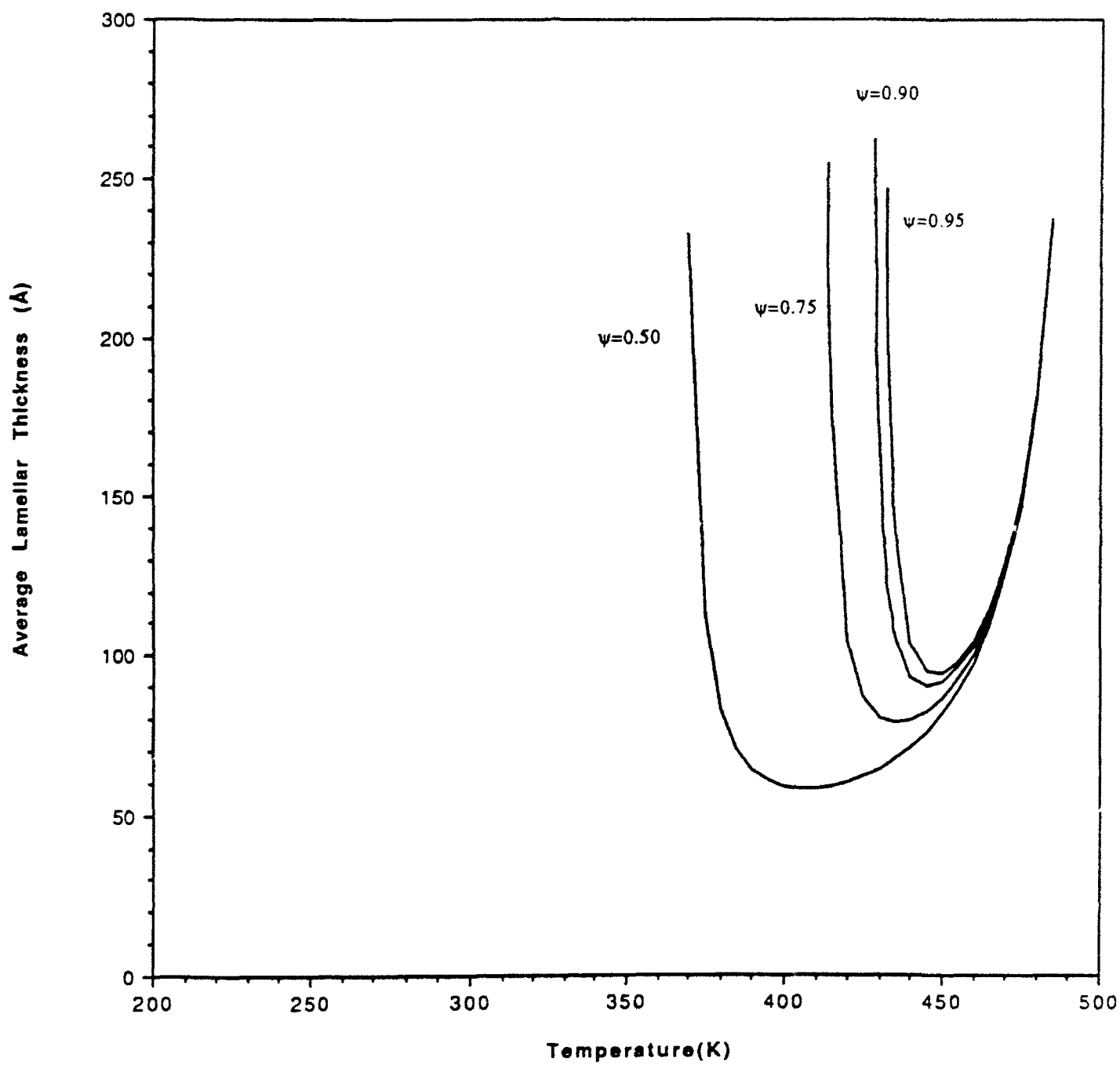


Figure 3(b).

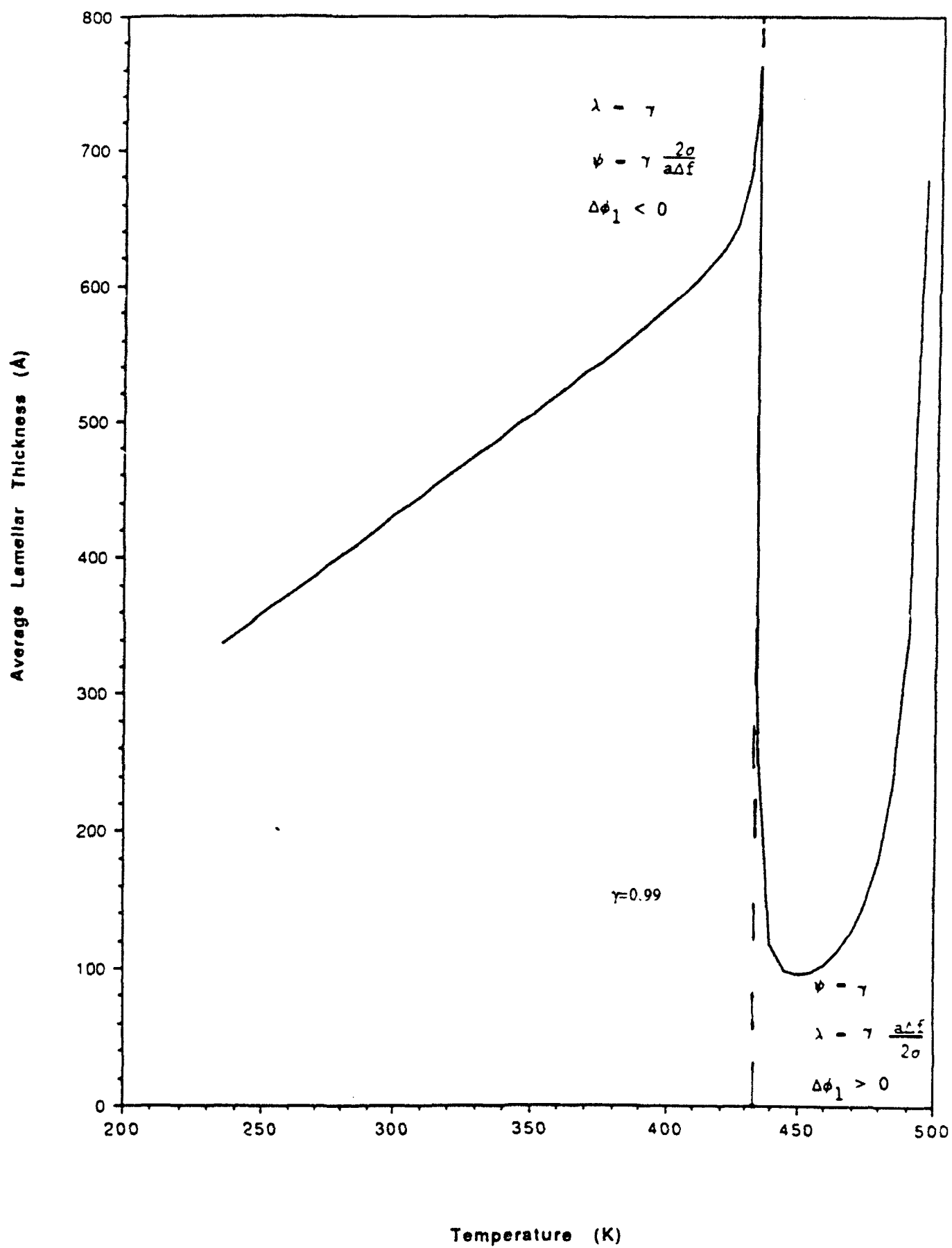


Figure 4.

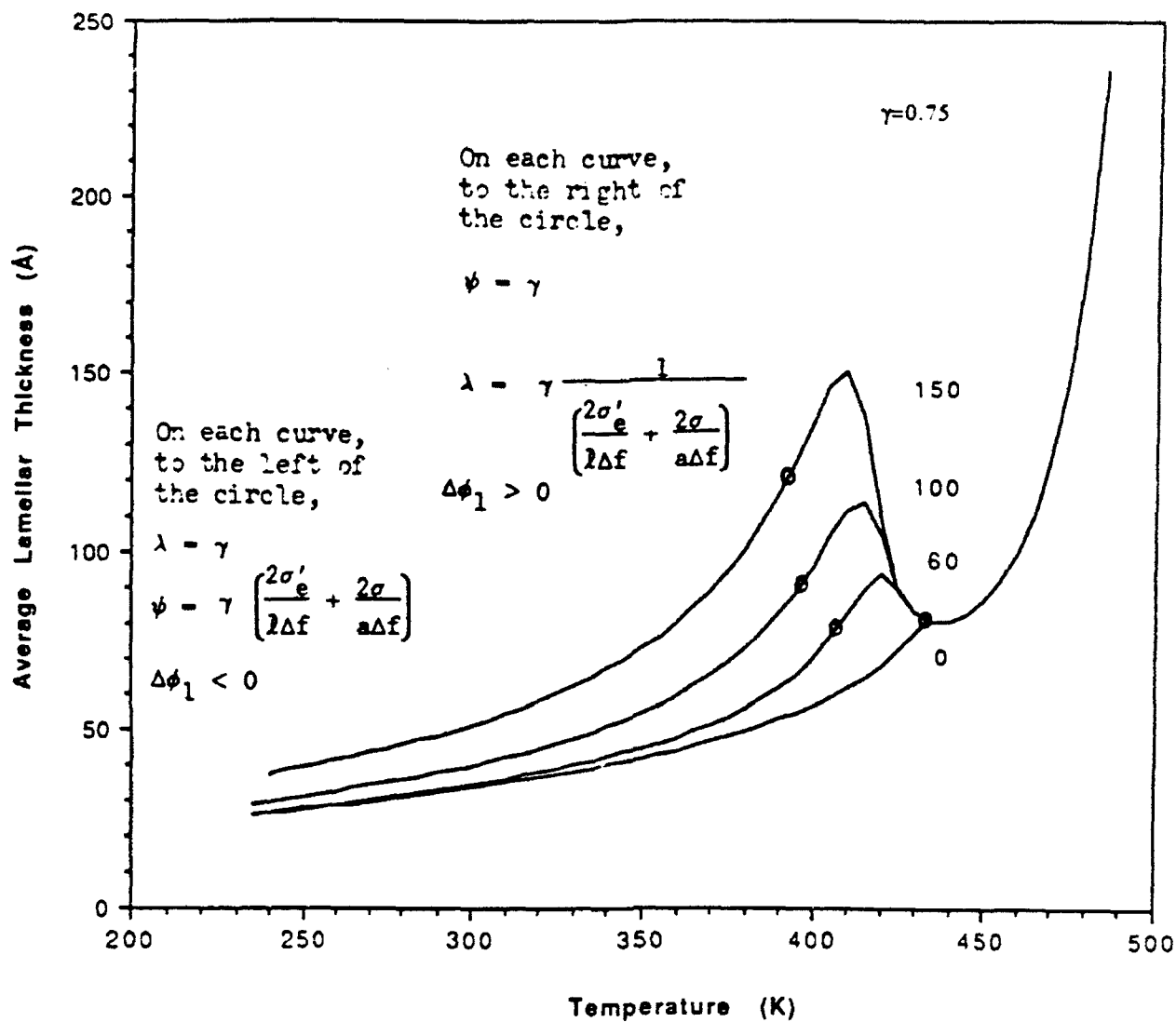


Figure 5.

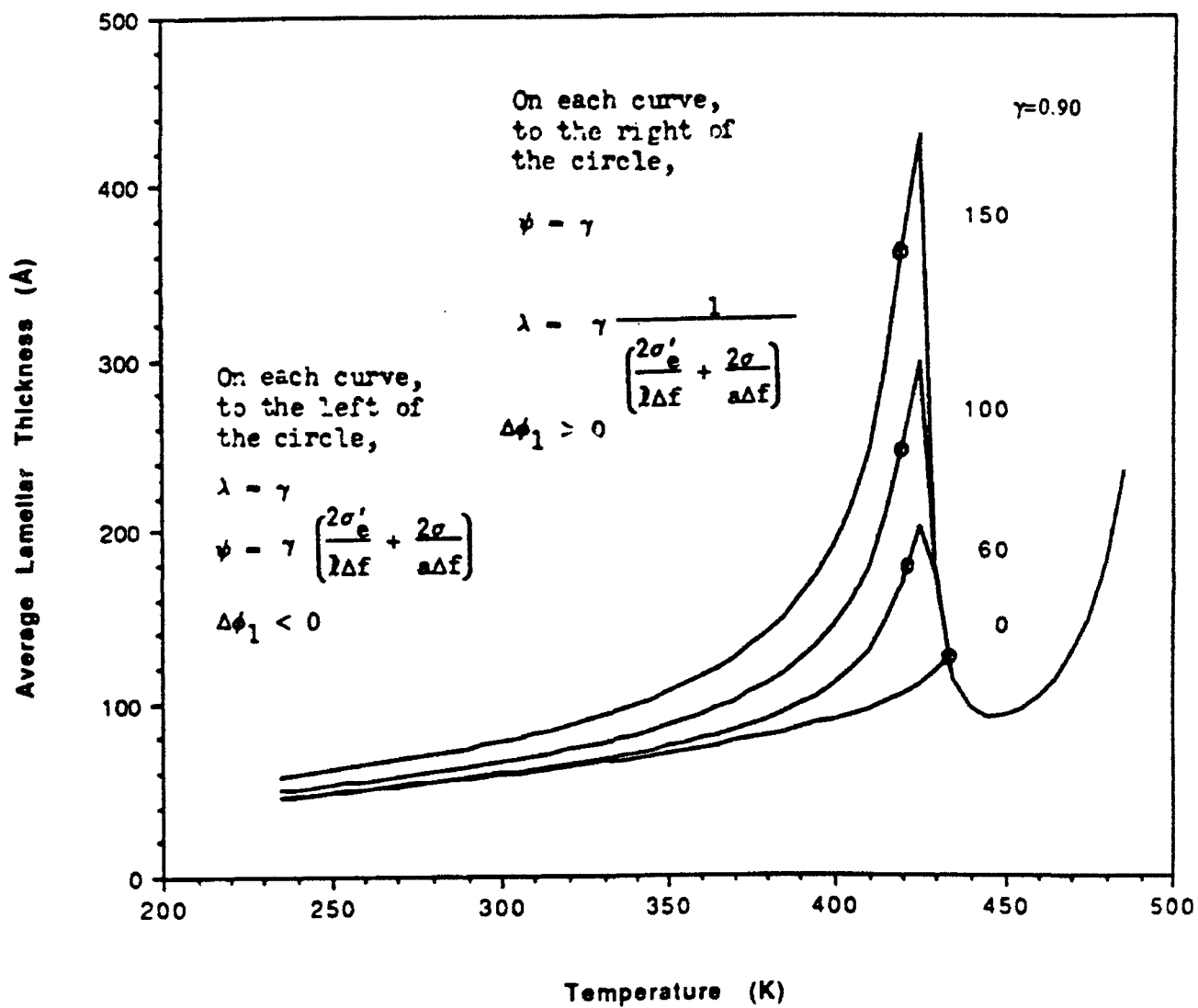


Figure 6.

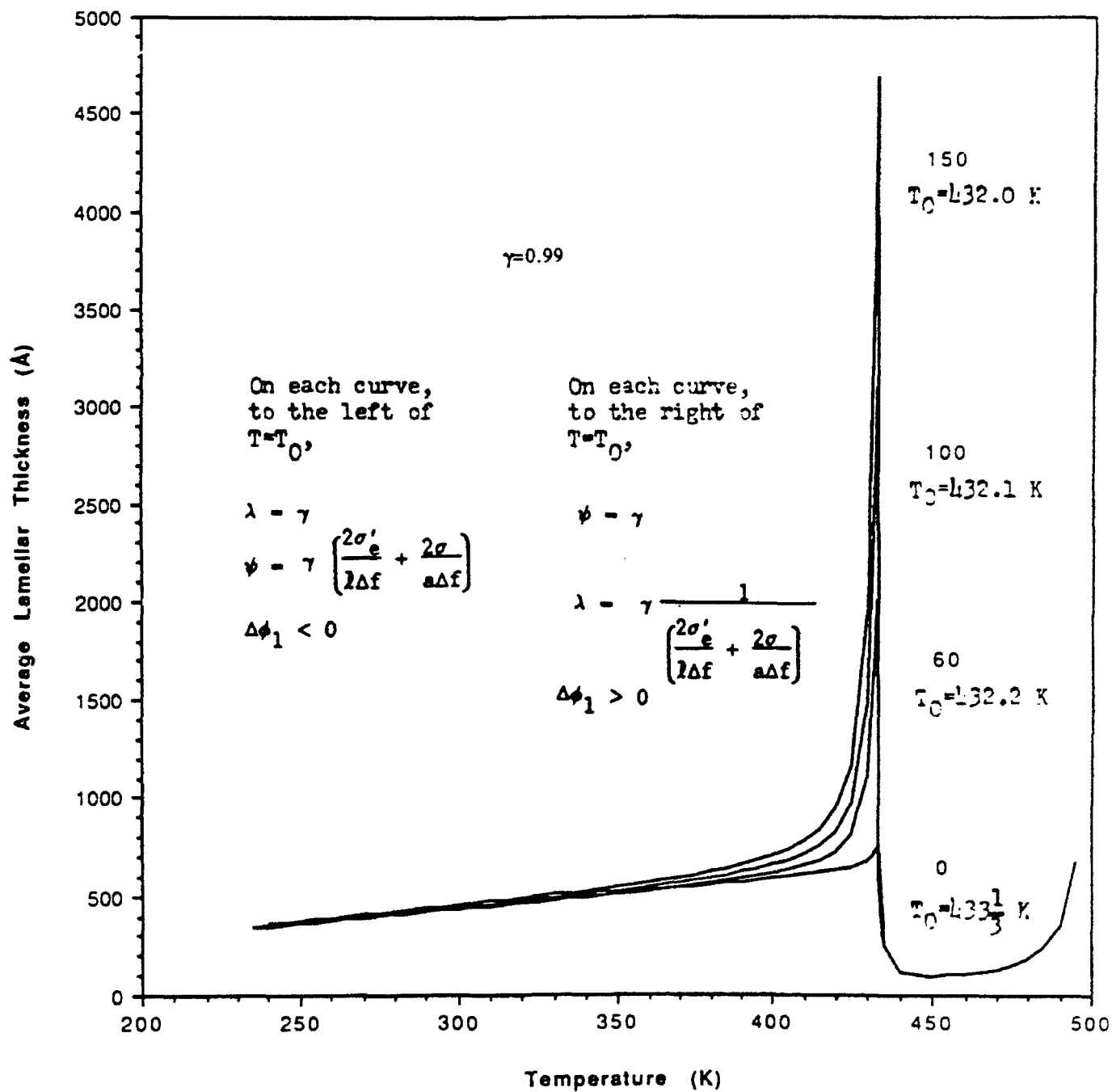


Figure 7.

Table I. Average Lamellar Thickness (Å)
vs. Temperature (K)

TEMP. (K)	Psi=Gamma=0	Gamma=1/2
485.000	234.383	235.303
480.000	178.390	179.781
475.000	144.660	146.556
470.000	122.074	124.507
465.000	105.867	108.867
460.000	93.652	97.253
455.000	84.105	88.342
450.000	76.429	81.344
445.000	70.115	75.762
440.000	64.826	71.267
435.000	60.328	67.641
430.000	56.451	63.528
425.000	53.072	59.481
420.000	50.100	55.988
415.000	47.463	52.941
410.000	45.105	50.259
405.000	42.984	47.877
400.000	41.064	45.744
395.000	39.316	43.821
390.000	37.718	42.077
385.000	36.251	40.484
380.000	34.897	39.023
375.000	33.644	37.676
370.000	32.480	36.429
365.000	31.396	35.270
360.000	30.382	34.188
355.000	29.433	33.176
350.000	28.540	32.225
345.000	27.700	31.329
340.000	26.907	30.484
335.000	26.157	29.683
330.000	25.446	28.924
325.000	24.772	28.201
320.000	24.130	27.513
315.000	23.518	26.855
310.000	22.935	26.226
305.000	22.377	25.624
300.000	21.843	25.045
295.000	21.332	24.489
290.000	20.841	23.953
285.000	20.369	23.437
280.000	19.915	22.938
275.000	19.479	22.456
270.000	19.057	21.990
265.000	18.651	21.537
260.000	18.258	21.099
255.000	17.878	20.673
250.000	17.511	20.259
245.000	17.155	19.856
240.000	16.809	19.463
235.000	16.475	19.081

Table II. Average Lamellar Thickness (\AA) vs. Temperature (K)

TEMP. (K) LH Psi=1/2

485.000	235.785
480.000	180.224
475.000	146.926
470.000	124.780
465.000	109.027
460.000	97.290
455.000	88.251
450.000	81.124
445.000	75.412
440.000	70.789
435.000	67.037
430.000	64.009
425.000	61.610
420.000	59.786
415.000	58.519
410.000	57.832
405.000	57.800
400.000	58.577
395.000	60.458
390.000	64.019
385.000	70.494
380.000	82.999
375.000	112.171
370.000	232.547
365.000	∞

Table III. Average Lamellar Thickness (\bar{L}) vs. Temperature (K)

TEMP. (K)	Theta=1 Gamma=1/2
495.000	675.848
490.000	
485.000	230.877
480.000	
475.000	142.184
470.000	
465.000	104.542
460.000	
455.000	84.037
450.000	
445.000	71.460
440.000	
435.000	63.333
430.000	
425.000	56.368
420.000	
415.000	50.779
410.000	
405.000	46.332
400.000	
395.000	42.690
390.000	
385.000	39.639
380.000	
375.000	37.036
370.000	
365.000	34.779
360.000	
355.000	32.796
350.000	
345.000	31.035
340.000	
335.000	29.454
330.000	
325.000	28.022
320.000	
315.000	26.716
310.000	
305.000	25.516
300.000	
295.000	24.405
290.000	
285.000	23.373
280.000	
275.000	22.407
270.000	
265.000	21.501
260.000	
255.000	20.646
250.000	
245.000	19.836
240.000	
235.000	19.067

Table IV. Average Lamellar Thickness (\bar{L}) vs. Temperature (K)

Gamma σ'_e

TEMP. (K) 0.5 // 60 0.5 // 100 0.5 // 150

485.000	235.303	235.303	235.303
480.000	179.781	179.781	179.781
475.000	146.556	146.556	146.556
470.000	124.507	124.507	124.507
465.000	108.867	108.867	108.867
460.000	97.253	97.253	97.253
455.000	88.342	88.342	88.342
450.000	81.344	81.344	81.344
445.000	75.762	75.762	75.762
440.000	71.267	71.267	71.267
435.000	67.641	67.641	67.641
430.000	64.735	64.735	64.735
425.000	62.454	62.454	62.454
420.000	60.723	60.743	60.743
415.000	59.214	59.577	59.584
410.000	57.306	58.874	59.005
405.000	54.856	58.337	58.984
400.000	52.149	57.582	59.533
395.000	49.469	56.411	60.296
390.000	46.971	54.852	60.919
385.000	44.708	53.035	61.120
380.000	42.683	51.095	60.800
375.000	40.874	49.136	60.003
370.000	39.252	47.220	58.842
365.000	37.791	45.385	57.434
360.000	36.466	43.648	55.882
355.000	35.253	42.015	54.261
350.000	34.136	40.486	52.625
345.000	33.100	39.056	51.009
340.000	32.131	37.719	49.436
335.000	31.219	36.468	47.918
330.000	30.358	35.295	46.462
325.000	29.541	34.194	45.072
320.000	28.766	33.159	43.746
315.000	28.028	32.183	42.485
310.000	27.324	31.262	41.286
305.000	26.652	30.390	40.145
300.000	26.009	29.564	39.059
295.000	25.392	28.778	38.025
290.000	24.799	28.031	37.040
285.000	24.229	27.318	36.101
280.000	23.681	26.637	35.204
275.000	23.152	25.985	34.346
270.000	22.641	25.360	33.526
265.000	22.147	24.760	32.740
260.000	21.669	24.184	31.986
255.000	21.206	23.628	31.263
250.000	20.756	23.093	30.567
245.000	20.320	22.576	29.898
240.000	19.896	22.076	29.253
235.000	19.484	21.593	28.631

Table V. Average Lamellar Thickness (\bar{R})
vs. Temperature (K)

TEMP. (K) Gamma=0.90

485.000	236.013
480.000	180.939
475.000	148.300
470.000	127.027
465.000	112.435
460.000	102.279
455.000	95.475
450.000	91.672
445.000	91.275
440.000	96.119
435.000	112.616
430.000	117.625
425.000	109.730
420.000	103.882
415.000	99.316
410.000	95.563
405.000	92.353
400.000	89.529
395.000	86.992
390.000	84.676
385.000	82.538
380.000	80.545
375.000	78.673
370.000	76.905
365.000	75.225
360.000	73.622
355.000	72.087
350.000	70.612
345.000	69.190
340.000	67.817
335.000	66.486
330.000	65.194
325.000	63.938
320.000	62.714
315.000	61.519
310.000	60.352
305.000	59.210
300.000	58.090
295.000	56.992
290.000	55.913
285.000	54.853
280.000	53.809
275.000	52.782
270.000	51.769
265.000	50.770
260.000	49.784
255.000	48.810
250.000	47.847
245.000	46.895
240.000	45.953
235.000	45.021

Table VI. Average Lamellar Thickness (\AA) vs. Temperature (K)

TEMP. (K) LH Psi=0.90

485.000	237.166
480.000	182.177
475.000	149.552
470.000	128.225
465.000	113.507
460.000	103.129
455.000	95.962
450.000	91.560
445.000	90.139
440.000	93.098
435.000	105.777
430.000	160.924
425.000	∞